Metallomics, 14, 2022, mfac061
https://doi.org/10.1093/mtomcs/mfac061
Advance access publication date: 26 August 2022
Paper

Comparative cisplatin reactivity towards human Zn_7-metallothionein-2 and MTF-1 zinc fingers: potential implications in anticancer drug resistance

Anjala W. Bulathge, Rhiza Lyne E. Villones, Fabian C. Herbert, Jeremiah J. Gassensmith and Gabriele Meloni*

Department of Chemistry and Biochemistry, The University of Texas at Dallas, 800 W Campbell Rd., Richardson, TX-75080, USA
*Correspondence: Gabriele Meloni, Department of Chemistry and Biochemistry, The University of Texas at Dallas, 800 W Campbell Rd., Richardson, TX-75080, USA. E-mail: gabriele.meloni@utdallas.edu

Abstract

Cis-diamminedichloroplatinum(II) (cisplatin) is a widely used metal-based chemotherapeutic drug for the treatment of cancers. However, intrinsic and acquired drug resistance limit the efficacy of cisplatin-based treatments. Increased production of intracellular thiol-rich molecules, in particular metallothioneins (MTs), which form stable coordination complexes with the electrophilic cisplatin, results in cisplatin sequestration leading to pre-target resistance. MT-1/-2 are overexpressed in cancer cells, and their expression is controlled by the metal response element (MRE)-binding transcription factor-1 (MTF-1), featuring six Cys_2His_2-type zinc fingers which, upon zinc metalation, recognize specific MRE sequences in the promoter region of MT genes triggering their expression. Cisplatin can efficiently react with protein metal binding sites featuring nucleophilic cysteine and/or histidine residues, including MTs and zinc fingers proteins, but the preferential reactivity towards specific targets with competing binding sites cannot be easily predicted. In this work, by *in vitro* competition reactions, we investigated the thermodynamic and kinetic preferential reactivity of cisplatin towards human Zn_7MT-2, each of the six MTF-1 zinc fingers, and the entire human MTF-1 zinc finger domain. By spectroscopic, spectrometric, and electrophoretic mobility shift assays (EMSA), we demonstrated that cisplatin preferentially reacts with Zn_7MT-2 to form Cys_4-Pt(II) complexes, resulting in zinc release from MT-2. Zinc transfer from MT-2 to the MTF-1 triggers MTF-1 metalation, activation, and binding to target MRE sequences, as demonstrated by EMSA with DNA oligonucleotides. The cisplatin-dependent MT-mediated MTF-1 activation leading to apo-MT overexpression potentially establishes one of the molecular mechanisms underlying the development and potentiation of MT-mediated pre-target resistance.

Graphical abstract

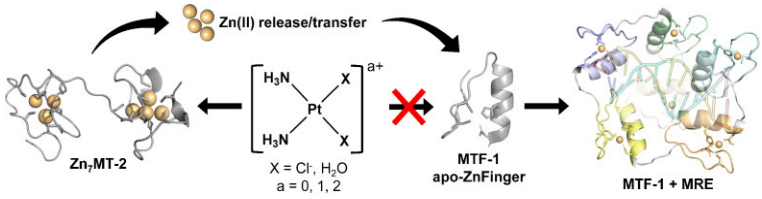

Cisplatin-dependent zinc transfer from MT-2 to MTF-1 triggers MTF-1 metalation, activation, and binding to MRE sequences

Introduction

Cis-diamminedichloroplatinum(II) (cisplatin) was the first inorganic antitumor drug introduced in clinics and among the most successful and intensively used chemotherapeutic agents for the treatment of testicular, ovarian, cervical, bladder, lung, and colorectal tumors.[1] Cisplatin was discovered in 1845 by Michele Peyrone, but its potential antineoplastic activity was revealed by Barnett Rosenberg in 1965.[2–4] The antitumor activity of cisplatin stems from its reactivity towards DNA.[5] Upon intravenous administration, due to the relatively high chloride concentration in plasma ([Cl^-] 100 mM), cisplatin remains inert and retains its Cl^- ligands. However, upon cellular uptake via passive diffusion or translocation via the copper transporter 1 (CTR-1)[6] or the organic cation transporters,[7] the cisplatin aquation reaction, in which the chloro ligands are substituted by H_2O/OH^- forming highly electrophilic mono- and di-aqua or -hydroxo di-amino complexes, spontaneously occurs in the cytoplasm as a consequence of the lower cytoplasmic chloride concentrations ([Cl^-] 2–10 mM).[1,5] These species react with DNA preferentially at the nucleophilic N-7 site of guanine residues to form intra-strand and inter-strand adducts introducing lesions and distortion in the DNA structure that cannot be efficiently repaired by DNA cellular repair mechanisms, subsequently leading to cancer cell apoptosis.[1,5] Though cisplatin is listed on the WHO's list of essential medicines and 50% of all patients who are treated by chemotherapy are administrated with cisplatin or other Pt(II) complexes, cisplatin use is restricted to reach its highest potential due to the intrinsic or acquired resistance that is developed in tumors cells after initial treatments.[6]

Received: March 25, 2022. **Accepted:** August 3, 2022

Cisplatin resistance can either be intrinsic to cells or acquired through exposure to the compound.[1,5] Diverse processes have been identified as potential responses leading to the resistance. These include changes in intracellular accumulation of the drug (changes in cisplatin import/export), increased production of intracellular thiols to prevent toxicity, and increased capability of cells to repair cisplatin-DNA damage.[1,8–10]

The resistance that stems from processes preceding the binding of cisplatin to its pharmacological target, DNA, is known as pre-target drug resistance.[1,8–10] Intracellular thiol-rich molecules, in particular glutathione (GSH) and metallothioneins (MTs), are prone to react and form stable coordination complexes with the highly electrophilic cisplatin aqua complexes, thereby sequestering and hindering cisplatin binding to mitochondrial and nuclear DNA.[10,11] Pt(II)-S bonds are thermodynamically very stable resulting in a competition between major intracellular thiols and DNA to react with the cisplatin,[12] with MTs showing a stronger Pt(II) scavenger effect compared to GSH.[11] Indeed, GSH was demonstrated to account for less than 20% of the Pt adducts formed intracellularly, when platinated species were isolated from cell extracts treated with cisplatin. Platinated adducts were primarily formed with higher MW (>3 kDa) biomolecules.[12] As the concentrations of reduced thiols in the high molecular mass fraction of the extracts was six times higher than in the low molecular fraction with MW <3 kDa, and considering MTs cysteine thiolate content (20 Cys residues/MT molecule), it can be expected that MTs are contributors to the thiolate-based Pt(II)-scavenging ability observed in cells.

Human MTs are small (61–68 aa) cysteine- and metal-rich proteins that play important roles in essential metal cellular physiology and metal buffering (Zn(II) and Cu(I)), as well as in metal detoxification (e.g. Cd(II)), potentially mediating the development of resistance to platinum-based anticancer drugs.[13–19] MTs can coordinate up to seven d^{10} divalent metal ions (Zn(II) and Cd(II)) into two metal-thiolate clusters via an array of 20 conserved cysteine residues, within two separate domains.[13,14,17,20–24] In fully metalated MTs, a $M(II)_3CysS_9$ cluster is assembled in the N-terminal β-domain and a $M(II)_4CysS_{11}$ cluster is formed in the C-terminal α-domain.[13–19] In each cluster, all divalent metal ions (Zn(II) or Cd(II)) are tetrahedrally coordinated by terminal and μ_2-bridging cysteine thiolates.[13,14,17,20–24] In humans, four MT isoforms (MT-1/-4) exist. MT-1 and MT-2 are ubiquitously expressed in high amounts in almost all tissues and organs.[14,17] Among all human isoforms, MT-2 shows the strongest Zn-thionein character, and play key roles in cellular zinc buffering and homeostasis under physiological conditions.[25–29] MT-1/2 have been detected in cellular cytoplasm, blood serum, and organelles, such as mitochondria, lysosomes, and in the nuclei of different cell types, playing varied roles in cell proliferation, differentiation, genotoxicity, and cell apoptosis.[30] MT-2 can translocate through the organelle membranes, and under oxidative stress can rapidly localize in the nucleus upon transport through nuclear pores.[31] In contrast to MT-3/-4, the biosynthesis of MT-1/-2 is inducible by hormones, cytokines, and metal ions.[14,17] Preclinical evidence shows that cells transfected with MT are more resistant to cisplatin, while clinical investigations demonstrated that in patients who are not responding to cisplatin, their basal MT levels are significantly elevated, they possess increased metastatic potential, and have shorter survival rates. Moreover, increased MT-2 levels have been observed in the nucleus of malignant tumors and nuclear MT-2 localization correlates with cisplatin resistance and poor clinical ramification.[32–44] Thus, high levels of MT expression in cancer cells correlate with acquired cisplatin resistance.[45] In addition, *in vitro* studies demonstrating the reactivity between Zn_7MTs and Pt(II) complexes or platinated DNA adducts further corroborate the important role of MTs in development of cellular resistance against platinum-induced toxicity.[46–53] However, the molecular mechanism of MT-mediated resistance remains to be fully elucidated as the processes leading to MT overexpression upon cisplatin administration are poorly characterized. One of the most potent inducers of MT biosynthesis are metal ions.[14,17,54,55] The transcriptional induction of MT genes is mediated by zinc binding to the metal-responsive transcription factor (MTF-1).[56,57] MTF-1 was first cloned from mice, and the human MTF-1 homologue is a 753-amino acid, 81-kDa protein with six TFIIIA-like Cys_2His_2 zinc fingers (ZnFs) in its N-terminal half.[56,58] Zinc binding to postulated sensory zinc-fingers in the six-finger domain, leading to full metalation, triggers MTF-1 activation, resulting in binding to specific DNA recognition motifs termed metal-responsive elements (MREs).[57–63] MREs are *cis*-acting MREs constituted by a 12-base pair conserved sequence (consensus sequence: TGCRCNC) present in multiple copies in the promoter region upstream of MT genes. MTF-1 activation and binding to the MREs results in induction of MT expression in responses to cellular zinc concentrations,[57–64] and several investigations with electrophoretic mobility shift assays (EMSA), using nuclear and whole cell extracts upon supplementation or depletion of zinc, indicate that the DNA-binding activation of MTF-1 is half-maximal at a total zinc concentration of 2–3 μM.[65,66] The MTF-1 ZnF domain was demonstrated to be responsible for the zinc responsiveness of MTF-1.[65] The activation of MTF-1 by zinc could also be achieved as a consequence of zinc release from Zn_7MTs under conditions like oxidative stress or displacement by more thiophilic copper ions.[67]

We hypothesized that a possible mechanism underlying MT-mediated platinum resistance can arise by a dichotomic process in which: (i) Pt(II) binding displaces zinc in the structure of Zn_7MTs resulting in Pt(II) sequestration and (ii) the released Zn(II) can be transferred to the inactive, zinc-deficient MTF-1 leading to full metalation and activation, thereby initiating the transcription of apo-MTs (MT-1 and MT-2). Increased concentrations of metal-free apo-MTs would result in increased sequestration of platinum drugs and potentiate the cisplatin- and MT-dependent MTF-1 activation leading to MT-mediated resistance.

ZnFs are structurally diverse protein domains.[68] Their reactivity, selectivity, and metal binding affinity stem from (i) the Cys and His residues involved in Zn(II) coordination, (ii) their hydrophobic core and structure formation, and (iii) the residues responsible for inter- and intramolecular interactions.[68] As a soft acid, Pt(II) shows high affinity for sulfur and nitrogen donor ligands. While it has been demonstrated that cisplatin reacts efficiently with MT cysteine thiolates,[46,48] it can also efficiently react with the zinc binding sites in Cys_4-, Cys_3His_1-, and Cys_2His_2-type ZnF proteins.[69–75] Studies on model ZnFs indicate that the rate of zinc displacement follows the order $Cys_4 \sim Cys_3His_1 > Cys_2His_2$,[69] showing that zinc binding in tetrahedral coordination drives folding and activation. On the other hand, it has been shown that ZnF platination would result in structural distortion and inactivation because Pt(II) favors square planar complexes.[73–75] While Pt(II) binding with guanine-N7 (and potentially the imidazole side chain of histidines) can be thermodynamically favored as a function of the local microenvironment and local dielectric constant, and the binding affinity can be larger than thiols despite the high stability of the Pt(II)-S bond thus allowing DNA platination, the ligand replacement rates on Pt(II) complexes by thiols and thioether ligands can be faster than that of nitrogens on heteroaromatic functional groups.[76–78] Thus, Pt(II)-sulfur interactions can be kinetically preferred.[76] As a consequence, ligand migration events in which thioether-Pt(II) bonds are formed first and then substi-

tuted by N-containing ligands have been described.[76] In addition to these considerations, the kinetics of ligand exchange in Pt(II) complexes is driven by the *trans* effect, which quantifies the ability to labilize the leaving group in *trans* position of a specific ligand, which in magnitude follows the order:[79]

$$SR_2 > SO_3^{2-} > SC(NH_2)_2 \sim NO_2^- \sim SCN- > Br^- > Cl^- > \text{pyridine} > NH_3 > OH^- \sim H_2O$$

Since the *trans* effect of thiols and thioethers is significantly larger than of the amine ligands of cisplatin, the labilization of amine ligands in *trans* position to thiols upon initial substitution of the leaving H_2O/OH^- ligands facilitates the subsequent formation of $Pt(II)S_4$ complexes in thiol-rich molecules such as MTs.[46] Based on these coordination chemistry considerations, it remains a challenge to determine a priori which platinated species are preferentially formed when multiple competing platination sites are present in metalloprotein mixtures.

In this work, we investigated the cisplatin reactivity towards each of the six individual ZnF motifs of human MTF-1, the entire MTF-1 six ZnF domain, and Zn_7MT-2, and studied the competitive reaction of cisplatin between MTF-1 and MT-2. The results revealed that cisplatin preferentially reacts with MT-2 to form Cys_4-Pt(II) complexes compared to MTF-1 ZnFs and that a cisplatin-dependent zinc transfer from MT-2 to the apo ZnFs is thermodynamically and kinetically favored, thus proving a potential mechanism for the cisplatin-dependent metal-exchange between Zn_7MT-2 and MTF-1 ZnFs. We also reveal that the cisplatin-dependent zinc transfer from MT-2 to the six ZnF domain of MTF-1 results in MTF-1 activation and its ability to bind to the target MRE sequence on DNA, thus potentially activating apo-MT expression. These results support a potential molecular mechanism underlying development of MT-mediated pre-target resistance that goes beyond the simple cisplatin sequestration that prevent Pt(II) reactivity towards DNA.

Material and methods

Expression, purification, and metal reconstitution of human metallothionein-2 (*h*MT-2)

The sequence encoding human MT-2 DNA (*h*MT-2) was synthetically prepared by codon optimization (Genscript Inc.) and cloned into pET-3d plasmid (Novagen) for recombinant expression. The resulting plasmid pET-3d-*h*MT2 was transformed into competent *Escherichia coli* BL21(DE3) pLysS cells. *h*MT-2 was expressed and purified as described in Faller *et al.*[80] *h*MT-2 was expressed in Cd-bound form by adding 0.4 mM $CdSO_4$ at 25°C, 30 min after the induction by IPTG (0.5 mM). Briefly, after cell lysis and differential ethanol precipitation steps, *h*MT-2 was purified by size exclusion chromatography (SEC) and anion exchange chromatography. The sample containing *h*MT-2 was loaded onto a gel filtration column (Superdex 75 HiLoad 26/600, GE Healthcare) and equilibrated with 25 mM Tris/HCl pH = 8, 50 mM NaCl and the protein eluted with the same buffer. The anion exchange chromatography was performed on a HiPrep DEAE FF 16/10 column connected to an Äkta Pure chromatographic system (GE Healthcare Life Sciences) equilibrated in 15 mM Tris pH = 8.6. *h*MT-2 was eluted with a linear salt gradient from 0 to 200 mM NaCl in 15 mM Tris pH = 8.6 at a flowrate of 8 ml/min and the protein recovered in the fraction eluted at ~50 mM NaCl. In both steps, the fractions containing *h*MT-2 were identified and pooled upon Cd(II) quantification via inductively coupled plasma-mass spectrometry (ICP-MS). The apo-*h*MT-2 was generated and Zn_7MT-2 was prepared by reconstitution using the method of Vašák.[81] The apo-protein was generated by purging the solution containing Cd-bound *h*MT-2 through N_2 bubbling followed by adjusting the pH to 1.5-2.0 via dropwise addition of concentrated HCl (6 M, purged with N_2 gas for 20 min) in the presence of guanidine-HCl (2 M) and the reducing agent dithiothreitol (DTT; 20 times in excess over the thiols concentration). The free metals were removed by SEC on a HiPrep 26/10 desalting column (GE Healthcare) connected to an Äkta Pure chromatographic system using 10 mM HCl for elution. The apo-*h*MT-2 concentration was determined by measuring the absorbance at 220 nm (ε_{220} = 48 200 M^{-1} cm^{-1}) in 0.1 M HCl on a Cary 300 UV-Vis spectrophotometer (Agilent).[29] Reconstitution to the Zn_7MT-2 form was performed by addition of 8 eq. $ZnCl_2$ followed by a slow adjustment of pH to 8.0 using 1 M Tris. Chelex 100 resin (10 mg/ml) was added to remove any unbound or weakly bound zinc, and then the resin was filtered from the protein solution using a 0.45 μm vacuum filter unit. A final SEC step was conducted using a Superdex 75 10/300 column to generate the reconstituted Zn_7MT-2 in 10 mM HEPES/HCl pH = 7.4, 100 mM $NaClO_4$ and to remove any low molecular weight contaminants. Protein purity was assessed by SDS-PAGE upon cysteine modification with monobromobimane following the method of Meloni *et al.*[82] The protein concentration was quantified photometrically in 0.1 M HCl using ε_{220} = 48 200 M^{-1} cm^{-1} (Cary 300 UV-Vis Spectrophotometer, Agilent). Thiol-to-protein ratios were determined by quantifying the concentration of free thiols upon their reaction with 2,2'-dithiodipyridine in 0.2 M sodium acetate, 1 mM EDTA (pH 4.0) using ε_{343} = 7600 M^{-1} cm^{-1}.[83] The zinc content was determined by ICP-MS (Agilent 7900, equipped with an autosampler) on samples digested in 50% (v/v) HNO_3 and diluted to final 2% (v/v) HNO_3 and Zn-to-protein ratios were calculated.

Preparation of MTF-1 apo zinc fingers (apo-ZnF-1/-6)

N-terminally acetylated and C-terminally amidated peptides corresponding to each of the MTF-1 six ZnFs (named ZnF-1/-6) were obtained by standard solid-phase peptide synthesis (GL Biochem, China). All the solutions utilized in the apo-ZnF preparation were rendered oxygen-free by at least three vacuum/nitrogen cycles on a Schlenk-line and transferred to a constant-flow nitrogen-purged glove box prior to sample preparation. For each apo-ZnF stock, 10 mg of each peptide was dissolved in 10 mM Tris/HCl pH = 8, 5 mM DTT. Samples were subsequently incubated for 1 h at 4°C to ensure complete reduction of the Cys residues. After incubation, the buffer was exchanged by passing the sample to a gel filtration column (HiTrap desalting 5 ml) equilibrated with 10 mM HEPES/HCl pH = 7.4, 100 mM $NaClO_4$ to remove DTT, Tris, residual trifluoroacetic acid, and to exchange Cl^- with ClO_4^-. The peptide corresponding to ZnF-5 proved to be extremely susceptible to cysteine oxidation and oligomerization above neutral pH when prepared with the described procedure. Therefore, to prepare the apo-ZnF-5, 10 mg of purified peptide was dissolved in oxygen-free 25 mM sodium acetate pH = 5, 10 mM TCEP to prevent oxidation. Prior to each reaction experiment, apo-ZnF-5 was rebuffered in oxygen-free buffer solutions (10 mM HEPES/HCl pH = 7.4, 100 mM $NaClO_4$) prepared by at least three vacuum/nitrogen cycles on a Schlenk-line and reactions were conducted in anaerobic conditions in a N_2-purged glove box. Thiol-to-protein ratios were determined by quantifying the stock peptide concentrations photometrically in 0.1 M HCl (Cary 300 UV-Vis Spectrophotometer, Agilent) using $\varepsilon_{280\,nm}$ = 2980 M^{-1} cm^{-1} for ZF-1, $\varepsilon_{280\,nm}$ = 1490 M^{-1} cm^{-1} for ZF-2/-3/-4/-6, and $\varepsilon_{260\,nm}$ = 400 M^{-1} cm^{-1} for ZnF-5 (using

extinction coefficients for Tyr at 280 nm and Phe at 260 nm), while the concentration of free thiols was determined upon their reaction with 2,2'-dithiodipyridine in 0.2 M sodium acetate, 1 mM EDTA (pH 4.0) using $\varepsilon_{343} = 7600\ M^{-1}\ cm^{-1}$.[83]

Zinc finger reconstitution with Zn^{2+} (holo-ZnF-1/-6)

All the solutions used for Zn^{2+} reconstitution of ZnF-1/-6 were rendered oxygen free by at least three vacuum/nitrogen cycles on a Schlenk-line. A total of 10 mg of each peptide was dissolved in oxygen-free 10 mM Tris/HCl pH = 8, 5 mM DTT inside a nitrogen-purged glove box. The samples were incubated for 1 h at 4°C. HCl was then added to a final concentration of 100 mM and samples were desalted using a HiTrap desalting column equilibrated and eluted with 10 mM HCl. To the peptide containing fractions, two equivalents of Zn^{2+} was added from a $ZnCl_2$ stock solution in water, followed by addition of 1 M Tris/HCl pH = 8 to a final concentration of 100 mM. The buffer was exchanged by passing the samples to a gel filtration column (HiTrap desalting 5 ml) equilibrated with 10 mM HEPES/HCl pH = 7.4, 100 mM $NaClO_4$ to remove unbound Zn^{2+} and Tris, and to exchange Cl^- with ClO_4^-. The monodispersity of the reconstituted holo-ZnF peptides was verified by injecting a sample of each holo-ZnF on a Superdex 75 10/300 GL column connected to an Äkta Pure chromatographic system and eluted with 10 mM HEPES/HCl pH = 7.4, 100 mM $NaClO_4$. Peptide concentrations were determined photometrically in 0.1 M HCl (Cary 300 UV-Vis Spectrophotometer, Agilent) using $\varepsilon_{280\ nm} = 2980\ M^{-1}\ cm^{-1}$ for ZF-1, $\varepsilon_{280\ nm} = 1490\ M^{-1}\ cm^{-1}$ for ZF-2/-3/-4/-6, and $\varepsilon_{260\ nm} = 400\ M^{-1}\ cm^{-1}$ for ZnF-5. Thiol-to-protein ratios were determined by quantifying the concentration of free thiols upon their reaction with 2,2'-dithiodipyridine in 0.2 M sodium acetate, 1 mM EDTA (pH 4.0) using $\varepsilon_{343} = 7600\ M^{-1}\ cm^{-1}$.[83] Zn-to-protein ratios were determined by quantifying the zinc content by ICP-MS (Agilent 7900) on samples digested in 50% (v/v) HNO_3 at 80°C and diluted to final 2% HNO_3 (v/v). The purity of holo-ZnF-1/-6 was also verified by SDS-PAGE.

Expression and purification of the six ZnF domain of human MTF-1 (*h*MTF-1-*zf*-domain)

For recombinant expression, the synthetic DNA (Genscript Inc.) encoding a codon-optimized ZnF domain of human MTF-1 featuring all six ZnFs (amino acids 140-314; Uniprot access number: Q14872; called *h*MTF-1-*zf*-domain throughout the manuscript) was cloned into a pET-52b(+) vector with an N-terminal STREP-tag II and a stop codon right downstream of ZnF-6 sequence.

The expression plasmid was transformed into *E. coli* BL21Gold(DE3) competent cells (Agilent Technologies). Cells were grown in Terrific Broth (TB) media supplemented with 1% glycerol (v/v) and ampicillin (50 μg/ml). The overnight preculture was inoculated in fresh TB media and cells were grown at 37°C under agitation until they reached OD_{600} = 1.2–1.6. Cells were cooled to 20°C, and protein expression was induced by adding isopropyl thiogalactopyranoside (IPTG) to a final concentration of 0.5 mM. After induction, cell cultures were also supplemented with $ZnCl_2$ to a final concentration of 100 μM. Cell cultures were subsequently incubated at 20°C, under agitation for 18 h.

Cells were harvested by centrifugation (20 min, 4°C, 15000 × g; Thermo Scientific Sorvall LYNX 6000 centrifuge) and resuspended in lysis buffer supplemented with zinc (25 mM Tris/HCl pH = 8, 300 mM NaCl, 5 mM $MgCl_2$, 100 μM $ZnCl_2$, 5 mM TCEP, 30 μg/ml deoxyribonuclease I from bovine pancreas (Sigma-Aldrich)) and with 1x EDTA-free protease inhibitor cocktail tablet (Thermo Scientific). Cells were lysed in an ice-cold microfluidizer at 20 000 psi by circulating the cell suspension three times through a Z-shaped diamond chamber (Microfluidics M-110P). Cell debris was removed by centrifugation (20 min, 4°C, 15000 × g; Thermo Scientific Sorvall LYNX 6000 centrifuge). The supernatant containing zinc-bound holo-*h*MTF-1-*zf*-domain was loaded onto a pre-equilibrated 5 ml StrepTrap column in wash buffer (20 mM Tris/HCl, pH = 8, 300 mM NaCl, 5 mM TCEP, 100 μM $ZnCl_2$) using an Äkta Pure FPLC system (GE Healthcare). The column was washed with 20-40 column volumes (CV) of buffer. *h*MTF-1-*zf*-domain bound to StrepTrap column was eluted with 6 CV (30 ml) buffer containing D-desthiobiotin (20 mM Tris/HCl pH = 8, 300 mM NaCl, 5 mM TCEP, 100 μM $ZnCl_2$). To remove desthiobiotin and free zinc, the sample was loaded on a dialysis bag and buffer exchanged via dialysis overnight into 10 mM HEPES/HCl pH = 7.4, 100 mM $NaClO_4$. Protein purity was verified by SDS-PAGE (using Mini-Protean TGX 4-15% precast polyacrylamide gradient gels from BioRad) and concentration was determined by measuring the absorbance at 280 nm (ε_{280} = 10 430 $M^{-1}\ cm^{-1}$). Thiol-to-protein ratios were determined by quantifying the concentration of free thiols upon their reaction with 2,2'-dithiodipyridine in 0.2 M sodium acetate, 1 mM EDTA (pH 4.0) using $\varepsilon_{343} = 7600\ M^{-1}\ cm^{-1}$.[83] Zn-to-protein ratios were determined by quantifying the zinc content by ICP-MS (Agilent 7900) on samples digested in 50% (v/v) HNO_3 at 80 ^{0}C and diluted to final 2% (v/v) HNO_3. The mass of the purified *h*MTF-1-*zf*-domain was also verified with matrix-assisted laser desorption/ionization (MALDI) mass spectrometry using cyano-4-hydroxycinnamic acid (CHCA) as matrix. Samples were analyzed using an AXIMA Confidence MALDI-TOF, from Shimadzu Biotech. All samples were combined with two layers of matrix and ran on the linear-negative mode. We used tobacco-mosaic virus (17 kDa) as calibrant for our analysis.

Apo-*h*MTF-1-*zf*-domain was generated by incubating the purified holo-*h*MTF-1-*zf*-domain in 1 mM EDTA, 5 mM TCEP for 60 min. The Zn-EDTA complex was removed by dialysis overnight into 10 mM HEPES/HCl pH = 7.4, 100 mM $NaClO_4$ in N_2-saturated buffer at 4°C. Thiol-to-protein ratios were determined by quantifying the concentration of free thiols upon their reaction with 2,2-dithiodipyridine in 0.2 M sodium acetate/1 mM EDTA (pH = 4.0) using $\varepsilon_{343} = 7600\ M^{-1}\ cm^{-1}$. To verify the efficiency of Zn removal from holo-*h*MTF-1-ZF-1-6 to generate apo-*h*MTF-1-*zf*-domain, Zn-to-protein ratios were determined by quantifying the zinc content by ICP-MS (Agilent 7900) on samples digested in 50% (v/v) HNO_3 at 80°C and diluted to final 2% (v/v) HNO_3.

Competitive reaction between cisplatin, Zn_7MT-2, and apo-/holo-ZnFs or holo-*h*MTF-1-*zf*-domain

A cisplatin (*cis*-diamminedichloroplatinum(II)) stock solution (2 mM, pH ~ 5–6) was prepared in Chelex-treated Millipore Ultrapure water and incubated for 24 h at room temperature. Subsequently, the cisplatin stock solution, the apo- and holo-ZnF-1/-6, holo-*h*MTF-1-*zf*-domain, and Zn_7MT-2 stock solutions in 10 mM HEPES/HCl pH = 7.4, 100 mM $NaClO_4$ were rendered oxygen-free by at least three vacuum/nitrogen cycles on a Schlenk-line and transferred into nitrogen-purged glove box. Each individual ZnF or holo-*h*MTF-1-*zf*-domain (final concentration: 20 μM or 40 μM) was mixed with Zn_7MT-2 (final concentration: 20 μM or 40 μM), and the competition reactions initiated by cisplatin addition (final concentration: 20 μM or 40 μM) at a 1:1:1 molar ratio. Samples were subsequently incubated for 120 h at 37°C in sealed tubes in absence of light. To quantify the reaction products and determine the preferential binding of cisplatin to MT-2 or ZnFs in the com-

petition reaction, the MT-2/ZnFs mixtures were separated via size exclusion chromatography (SEC) based on their different molecular weight (MT-2: ~6.5 kDa; ZnFs ~3 kDa). 500 μL samples, taken from the reaction mixtures, were injected in a Superdex 75 10/300 GL column connected to an Äkta Pure chromatographic system and eluted with a 10 mM HEPES/HCl pH = 7.4, 100 mM $NaClO_4$. The fractions corresponding to MT-2 and ZnF were collected for Zn-/Pt-to-protein ratio determinations. Since ZnF-2 and ZnF-5 interacted with the Superdex 75 matrix in the SEC separation step, the reaction mixtures containing ZnF-2 and ZnF-5 were separated by ion exchange chromatography. A total of 500 μL samples were injected on a 1 ml HiTrap Q HP anion exchange column connected to an Äkta Pure chromatographic system in 25 mM Tris/HCl pH = 8, and eluted with a linear gradient (0–100%, 1 CV) utilizing 25 mM Tris/HCl pH = 8, 500 mM NaCl as second buffer solution. For the mixture containing *h*MTF-1-*zf*-domain, 500 μL samples were injected on a 1 ml Hitrap Q HP anion exchange column connected to an Äkta Pure chromatographic system in 10 mM HEPES/HCl pH = 7.4, and eluted with a linear gradient (0–100%, 1 CV) utilizing 10 mM HEPES/HCl pH = 7.4, 1 M $NaClO_4$ as second buffer solution.

As the development of sulfur-Pt(II) ligand-to-metal charge transfer (LMCT) transitions would interfere with photometric determination of peptide concentrations at 280 nm upon formation of Pt(II) complexes, ZnFs peptide concentrations were determined with the Pierce Quantitative Colorimetric Peptide Assay based on a modified BCA method, using the corresponding ZF stock solutions to generate a serial dilution calibration series for each peptide as a standard.

Zn-/Pt-to-ZnFs/MT-2 ratios were determined via quantification of total Zn and Pt by ICP-MS. Samples were digested in 50% (v/v) HNO_3 at 80°C for 16 h and diluted to final 2% (v/v) HNO_3 for ICP-MS analysis on an Agilent 7900 instrument equipped with an autosampler. For MT-2, the protein concentration was estimated from the metal determination by assuming a total of seven metal equivalents bound (Zn plus Pt) after the reaction, based on stoichiometric substitution of Zn(II) by Pt(II) as previously demonstrated.[46] As controls, to test whether cisplatin-independent zinc transfer can occur between Zn_7MT-2 and apo-ZnFs, similar experiments were conducted in the absence of cisplatin in the reaction mixtures.

Binding kinetics of cisplatin to MT-2 and apo-/holo-ZnFs

The kinetics of cisplatin binding to Zn_7MT-2, Zn^{2+}-bound ZnF-1/-6, and apo-ZnF-1/-6 were monitored by following the development of characteristic CysS-Pt(II) LMCT transitions by absorption spectroscopy. Zn_7MT-2, apo-ZnF-1/-6, and Zn^{2+}-ZnF-1/-6 in 10 mM HEPES/HCl pH = 7.4, 100 mM $NaClO_4$, and cisplatin stock solutions in H_2O were rendered oxygen-free by three freeze-nitrogen gas pump cycles on a Schlenk line and placed in a 4°C incubator inside a nitrogen-purged glove box. Zn_7MT-2 (20 μM), each holo-ZF-1/-6 (20 μM), or apo-ZF-1/-6 peptide (20 μM) were mixed at a final 1:1 stoichiometry (mol/mol) with cisplatin (from a 2 mM stock in H_2O, incubated for 24 h at room temperature) in 10 mM HEPES/HCl pH = 7.4, 100 mM $NaClO_4$. Samples were placed in 1 cm quartz cuvette and immediately sealed in inert atmosphere. Absorption kinetic traces at 285 nm were followed by UV-Vis absorption for 120 h at 37°C in a Cary 5000 spectrophotometer equipped with a Peltier thermostatic multicell holder. Kinetic traces were normalized by quantifying the amount of Pt(II)-S bonds formed in each sample based on the recorded absorbance as a function of time, using the CysS-Pt(II) LMCT absorption (ε_{285} = 2850 M^{-1} cm^{-1} per bond) for quantification.[46] For comparative purposes, the apparent relative velocities were extrapolated for each reaction by determining the Abs_{285} of the kinetic traces in the first 300 min of the reaction.

Determination of Zn^{2+} dissociation constants (K_D) for holo-ZnF-1/-6, Zn_7MT-2, and *h*MTF-1-*zf*-domain using 4-(2-pyridylazo) resorcinol (PAR)

ZnF-1-Zn^{2+}, ZnF-2-Zn^{2+}, ZnF-3-Zn^{2+}, ZnF-4-Zn^{2+}, ZnF-5-Zn^{2+}, and ZnF-6-Zn^{2+} reconstituted samples, Zn_7MT-2 and *h*MTF-1-*zf*-domain (final concentrations: 10 μM in 10 mM HEPES/HCl pH = 7.4, 100 mM $NaClO_4$) were rendered oxygen-free by three vacuum-nitrogen gas pump cycles and mixed with oxygen-free 4-(2-pyridylazo) resorcinol (final concentration: 20 μM) at 25°C for 24 h inside a constant-flow nitrogen-purged anaerobic glovebox. The concentration of the $ZnH_x(PAR)_2$ complex formed was subsequently determined by recording the electronic absorption spectra and the sample absorbance at 492 nm (ε_{492} = 71 500 M^{-1} cm^{-1}). The average dissociation constants K_D were calculated according to the following equations, using the effective dissociation constant of $ZnH_x(PAR)_2$ at pH 7.4 (K_d^{eff} = 7.08 × 10^{-13} M^2):[84]

$$P + ZnH_x(PAR)_2 \rightleftharpoons P - Zn + 2H_xPAR$$

$$K_{ex} = \frac{[H_xPAR]^2[P - Zn]}{[ZnH_x(PAR)_2][P]}$$

$$K_d^L = K_d^{eff} \times \frac{1}{K_{ex}}$$

Electrophoresis mobility shift assays

EMSAs were performed to detect *h*MTF-1-*zf*-domain—DNA (Zn_6MTF-1) interactions using a nucleotide containing the MRE sequence recognized by the hexa-ZnF domain of *h*MTF-1. A double-stranded oligonucleotide containing the MRE's sequence was synthetized (Genscript Inc.) and labeled with 6-carboxyfluorescein at the 5′-end. The selected oligonucleotide sequence used is given below (with bases of the MRE functional core highlighted in bold):[66]

5′-GATCCAGGGAGCTC**TGCAC**A**C**GGCCCGAAAAGTAGTCCCTC GAGACGTGTGCCGGGCTTTTCATCTAG-3′

Samples (1–4.2 μL) containing Zn_7MT-2 (0.50 mM, from a 0.93 mM stock in 10 mM HEPES/HCl pH = 7.4, 100 mM $NaClO_4$), Zn_6MTF-1 (10 μM, from a 40 μM stock in 25 mM Tris/HCl pH = 8, 300 mM NaCl, 1 mM TCEP, 100 μM $ZnCl_2$, 2.5 mM desthiobiotin), or Zn_6MTF-1 (10 μM) in the presence of EDTA (2.5 mM, from a 0.50 mM stock pH = 8) were mixed with 6FAM-labeled oligonucleotide (1 pmol and kept constant), and used in the assays as controls. Zn^{2+} MTF-1 titrations with (a) increasing EDTA concentrations (1–2.5 mM) and (b) 2.5 mM EDTA in the presence of increasing supplemented Zn^{2+} (0.50–5.0 mM, from a 100 mM $ZnCl_2$ stock) were tested to optimize the conditions to be used as negative and positive controls, respectively; EMSA performed on these samples were described in the corresponding figure legend found in the 'Results' section. Samples containing only the 6FAM-labled oligonucleotide (1 pmol) were used as standard where no shift is observed, as no protein is included in the sample. All samples were strictly incubated for 30 min at room temperature upon mixing prior to gel electrophoresis.

Table 1. List of peptides corresponding to each of the six *h*MTF-1 zinc fingers utilized in this study with corresponding theoretical molecular weights and experimentally determined mass (via ESI-MS)

Zn finger	Position	Length	Sequence	Theoretical mass (Da)	Experimental mass (Da)	ε_{280} (M^{-1} cm^{-1})
ZnF-1	140-164	25	Ac-YQCTFEGCPRTYSTAGNLRTHQKTH-NH_2	2941.23	2941.22	2980
ZnF-2	170-194	25	Ac-FVCNQEGCGKAFLTSYSLRIHVRVH-NH_2	2906.36	2906.34	1490
ZnF-3	200-224	25	Ac-FECDVQGCEKAFNTLYRLKAHQRLH NH_2	3048.47	3048.45	1490
ZnF-4	229-253	25	Ac-FNCESQGCSKYFTTLSDLRKHIRTH-NH_2	3013.38	3014.35	1490
ZnF-5	259-283	25	Ac-FRCDHDGCGKAFAASHHLKTHVRTH-NH_2	2873.21	2873.19	400 (ε_{260})
ZnF-6	289-313	25	Ac-FFCPSNGCEKTFSTQYSLKSHMKGH-NH_2	2906.29	2906.27	1490

The corresponding absorption extinction coefficients used to determine the peptide concentrations are listed. All peptides were N-terminally acetylated (Ac-) and C-terminally amidated (-NH_2).

A reaction mixture between Zn_7MT-2 and cisplatin 1:1 mol/mol (1 mM in in 10 mM HEPES/HCl pH = 7.4, 100 mM $NaClO_4$) was prepared in an anaerobic glove box and reacted for 120 h at 37°C. The reaction product was subsequently mixed to a final concentration of 0.5 mM, with Zn_6MTF-1 (10 μM) in the presence of EDTA (at a concentration that would prevent MTF-1 ability to bind DNA due to Zn removal from the ZnFs). Similarly, a sample in which Zn_6MTF-1 (10 μM final concentration) and Zn_7MT-2 (0.50 mM final concentration) were coincubated and reacted with cisplatin (0.50 mM) in an anaerobic glove box for 120 h at 37°C was mixed with 2.5 mM EDTA and 6FAM-labeled oligonucleotide prior to gel electrophoresis.

All samples containing DNA and/or protein–DNA complexes were mixed with native PAGE sample buffer (2–8 μL; BioRad) and separated by native polyacrylamide gel electrophoresis using Mini-Protean TGX 4–15% precast polyacrylamide gradient gels (BioRad) run at 160 V for 45 min using native running buffer (25 mM Tris pH = 8.3, 192 mM glycine). Gels were imaged using a BioRad ChemiDoc Touch imaging system over a transilluminating tray with excitation in visible wavelength region and equipped with filters for SYBR Green imaging (20 s exposure).

Results and Discussion

Determination of the preferential cisplatin reactivity between Zn_7MT-2 and apo-/holo-MTF-1 ZnFs

Reactivity and complex formation between cisplatin and proteins such as albumin, myoglobin, transferrin, cytochrome, MTs, and ZnFs, among others, revealed that cisplatin is primarily coordinated through Cys, His, or Met residues.[46,69–75,85–91] ZnF proteins have been reported to be targets of platination.[69–75] Because of the square planar coordination geometry, Pt(II) binding can severely affect the structure of ZnFs thus leading to protein inactivation. For example, the reaction of cisplatin with a 31-residue model peptide of DNA polymerase-α leads to irreversible cisplatin binding with consequent dramatic structural perturbations, suggesting the inhibition of transcription.[72] Accordingly, cisplatin binding to DNA polymerase-I results in unwinding of its ZnF domain upon formation of two reaction intermediates: a Pt-Zn-peptide complex and a bis-cysteine platinum complex.[74,75] Similarly, studies performed on the C-terminal ZnF of HIV-1 NCp7 proteins showed that reaction with platinum complexes leads to Zn(II) release from the peptide, resulting in loss of the ZnF tertiary structure.[70,92] Cisplatin reaction with the 18-residue Cys_3His_1 ZnF motif derived from a retroviral nucleocapsid protein PyrZf18 blocks the cysteine zinc binding ligands in the peptide and slowly ejects zinc from the zinc–peptide complex, leading to the formation of a complex in which three cysteines and one ammonia molecule are coordinated to platinum.[73] The reactivity of the ZnF domains with Pt(II) complexes depends on the type of zinc binding motifs (Cys_2His_2, Cys_3His_1, or Cys_4), the nature of the Pt(II) complex, and the specific ZnFs in cases of multi ZnF proteins. Cisplatin reaction with different types of ZnF motifs, including the second ZnF domain of the Sp1 transcription factor (Cys_2His_2), the second ZnF domain of the PARP-1 protein (Cys_3His_1), and the ZF domain of the MDM2 protein (Cys_4), revealed a faster cisplatin reaction towards Cys_3His_1 and Cys_4 ZnFs.[69] On the other hand, a differential ZnF reactivity towards Pt(II) complexes was observed in Sp1 transcription factor, in which the third ZnF domain was demonstrated to possess a higher reactivity towards cisplatin than the second ZnF domain.[71] These results indicate that the protein context around the zinc coordination sphere contributes to the modulation of cisplatin selectivity and reactivity with ZnF proteins. This is also in line with the notions that ZnFs possess different zinc affinities as well as reactivities at their metal binding sites, such as towards alkylation reactions as also exemplified by investigations on MTF-1.[93]

Thus, in this work, to study the comparative reactivity of cisplatin towards MTF-1 and Zn_7MT-2, we designed an approach in which individual peptides corresponding to the individual ZnFs of the hexa-ZnF domain of *h*MTF-1 were generated (Table 1) and compared their reactivity to the one towards Zn_7MT-2 (Fig. 1). N-terminally acetylated and C-terminally amidated peptides were synthetized by solid-phase synthesis and procedures for generating the apo- and Zn^{2+}-bound holo forms were developed. Throughout our investigation, we attempted to mimic physiological-like pH and ionic strength conditions, thus, the ZnFs and Zn_7MT-2 samples were prepared in 10 mM HEPES/HCl pH 7.4, in the presence of 100 mM ClO_4^-, which does not efficiently coordinate Pt(II).

Apo-ZnF-1/-6 peptides were generated in anaerobic atmosphere by treatment with an excess of reducing agent (DTT) followed by a desalting step to buffer each peptide stock in the reaction buffer and to remove any chloride trace for further investigation of cisplatin reactivity. Zn^{2+}-bound ZnF-1/-6 peptides were instead generated by initial treatment of the apo-peptides with an excess of reducing agent (DTT), followed by acid treatment to protect cysteine residues from oxidation during the zinc reconstitution procedure. Acidified apo-peptide stocks were incubated with an excess of Zn^{2+} (2:1 [Zn^{2+}]/[ZnF-1/-6] mol/mol) followed by a pH increase to obtain zinc binding to the Cys_2His_2 binding site. A subsequent desalting step was introduced to remove excess zinc and to buffer the holo-peptides in the reaction buffer. The monodispersity of all generated holo-peptides was confirmed by size exclusion chromatography (Fig. 2A and Supplementary Fig. 1) and the peptide purity was confirmed by SDS-PAGE (purity > 95%; Fig. 2B). Absence of cysteine oxidation in apo- and holo-peptides was confirmed by sulfhydryl group quantification and Cys-to-protein ratio determination (Table 2),

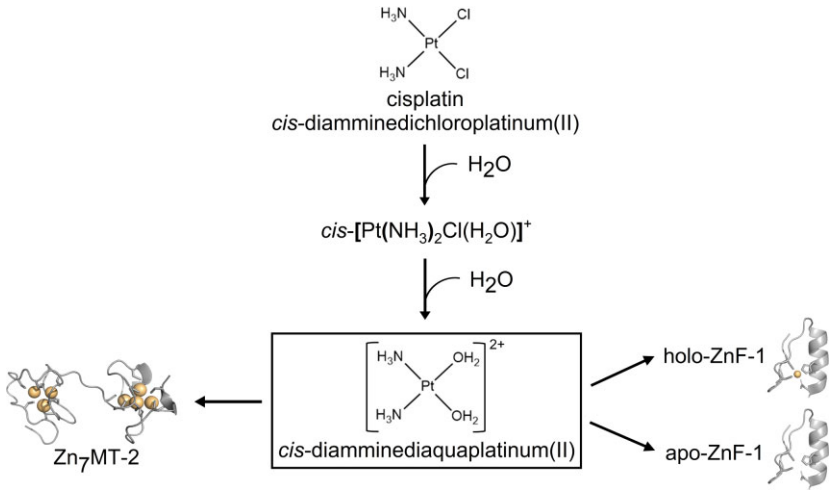

Fig. 1 Representative reactions of aquated cisplatin (diamminediaquaplatinum(II)) with Zn_7MT-2 or MTF-1 zinc fingers (ZnFs). Cisplatin reactions were carried out with either Zn_7MT-2 or holo-/apo-zinc fingers (ZnF-1 as shown) or in competition experiments in the presence of both Zn_7MT-2 and holo-/apo-zinc fingers. Models were generated using PyMol: the Zn_7MT-2 structure (with zinc ions shown as *light-yellow spheres*) is based on the X-ray crystal structure of rat Zn_2Cd_5MT-2 (PDB: 4MT2), while the human metal regulatory transcription factor 1 (MTF-1) ZnF-1 (corresponding to residues 140-164) was generated from the MTF-1 model coordinates deposited in the AlphaFold Protein Structure Database (AF-Q14872).

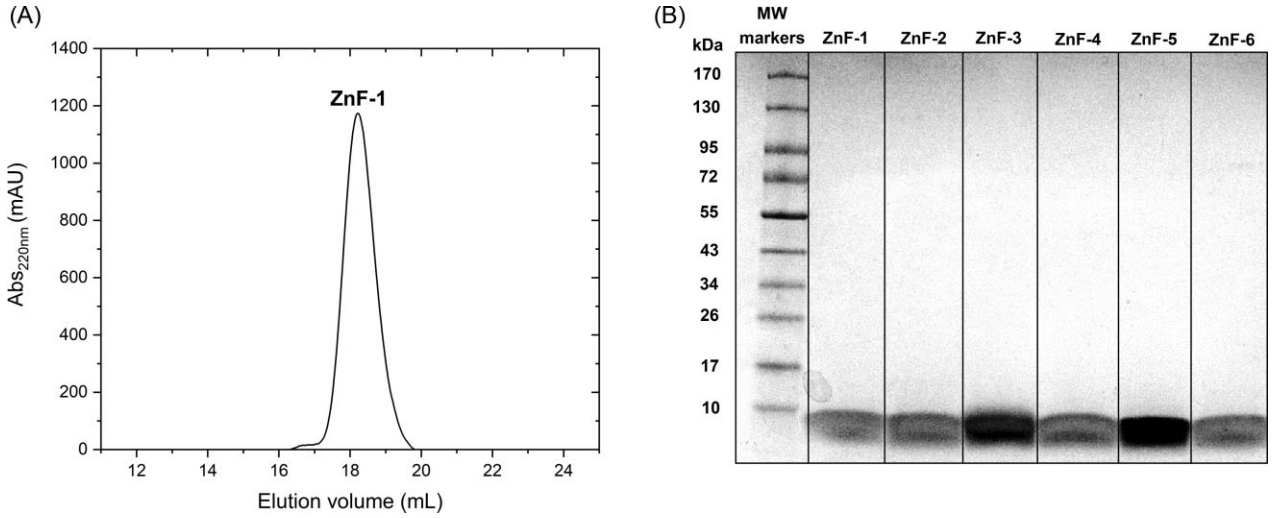

Fig. 2 Zinc reconstitution of individual *h*MTF-1 holo-zinc fingers (ZnF-1/-6). (A) Size exclusion chromatography elution profile of holo-ZnF-1 (representative, 20μM; see also Fig. S1) in 10 mM HEPES/HCl pH 7.4, 100 mM $NaClO_4$, revealing a monodispersed peak upon zinc reconstitution. (B) Purity of Zn-reconstituted holo-ZnF-1/-6 analyzed by SDS-PAGE and stained with Coomassie Blue.

while metal-to-protein ratios for each of the holo-peptides were determined upon zinc quantification (Table 2) by ICP-MS.

Zinc-to-protein ratios in Zn^{2+}-ZnF-1/-6 confirmed successful reconstitution and the binding of 1 Zn^{2+} equivalent to each of the fingers, and the obtained cysteine-to-peptide ratios (approximately 2:1 mol/mol) are consistent with the absence of significant cysteine oxidation. Similarly, absence of cysteine oxidation was confirmed in apo-ZnF peptide stocks (Table 2).

Similarly, recombinant human Zn_7MT-2 was generated by zinc reconstitution of the purified Cd-bound form using established procedures. The zinc-to-protein and Cys-to-protein ratios obtained after buffering the Zn_7MT-2 stocks in the reaction buffer are consistent with the successful generation of fully zinc-bound MT-2 without any cysteine oxidation (Table 2).

The competitive reaction between MTF-1 ZnFs and Zn_7MT-2 towards cisplatin was subsequently investigated by mixing equimolar concentrations of ZnF-1/-6 and Zn_7MT-2, and incubating the mixture in the presence of 1 equivalent of aquated cisplatin ($[Pt(NH_3)X_2]^{a+}$ (X = OH^- or H_2O; a = 0, 1, 2)). While the reaction kinetics between cisplatin and Zn_7MT-2 appear to be largely independent of the leaving ligand, as also observed in the case of the S-donor compounds cysteine and GSH, the exchange of the leaving ligand is an important step to activate the compounds for their reactions with N7-guanine, and thus potentially affecting its reactivity with the N-atoms in histidine side chains present in ZnFs.[53,94,95] The reactivity of cysteine and histidine ligands towards platination in ZnF metal binding sites is expected to differ in the presence or absence of zinc, and expected to be lower in holo-ZnFs in light of the presence of CysS-Zn(II) and HisN-Zn(II) bonds, which would slow the ligand exchange reactions with Pt(II) when compared to the free thiolates or imidazole ligands. We thus performed all the competition and reactivity

Table 2. Zinc-to-protein (mol/mol) and thiol-to-protein (mol/mol) ratios for the reconstituted Zn_7MT-2, apo- and holo-ZnF-1/-6, and apo- and holo-*h*MTF-1-*zf*-domain utilized in this work

Protein/peptide	[Zn]/[protein]	[SH]/[protein]
Zn_7MT-2	7.26 ± 0.12	19.92 ± 0.85
apo-ZnF-1	-	2.26 ± 0.40
apo-ZnF-2	-	2.30 ± 0.93
apo-ZnF-3	-	2.42 ± 0.23
apo-ZnF-4	-	2.56 ± 0.61
apo-ZnF-5	-	2.23 ± 0.80
apo-ZnF-6	-	2.32 ± 0.22
holo-ZnF-1	1.37 ± 0.08	2.33 ± 0.12
holo-ZnF-2	1.08 ± 0.08	2.10 ± 0.67
holo-ZnF-3	1.25 ± 0.23	2.05 ± 0.17
holo-ZnF-4	0.91 ± 0.06	2.11 ± 0.25
holo-ZnF-5	0.91 ± 0.02	2.12 ± 0.67
holo-ZnF-6	1.19 ± 0.04	2.56 ± 0.65
apo-*h*MTF-1-*zf*-domain	0.141 ± 0.002	10.11 ± 0.36
holo-*h*MTF-1-*zf*—domain	5.50 ± 0.23	10.69 ± 0.66

investigations throughout the study utilizing both apo- and holo-ZnFs, to address whether preferential reactivities between MT-2 and ZnFs are affected as a function of the occupation of their zinc binding site.

Reaction mixtures, each containing apo-ZnF and Zn_7MT-2, or holo-ZnFs and Zn_7MT-2, were prepared in anaerobic atmosphere and the competitive reaction with cisplatin was initiated by the addition of 1 Pt(II) equivalent. Reaction mixtures were incubated in 10 mM HEPES/HCl pH 7.4, 100 mM $NaClO_4$ at 37°C, in absence of light, for 120 h. After the reactions were completed, mixtures were collected to quantify metal speciation in MT-2 versus ZnF-1/-6. We separated each of the two components in each reaction mixture by size exclusion chromatography in light of the different size of MT-2 and ZnF peptides (Fig. 3 and Supplementary Figs 2–6), followed by Zn- and Pt-to-protein quantification in each of the MT-2 or ZnF purified fractions. As ZnF-2 and ZnF-5 appeared to partially interact with the matrix of the SEC column, reaction mixtures containing these peptides were separated via anion exchange chromatography prior to metal quantification.

Analysis of Pt-to-protein ratios at the end of the reaction revealed preferential Pt(II) binding to Zn_7MT-2 in case of all holo-ZnF peptides, with Pt(II)-to-MT-2 ratios approaching stochiometric ratios ([Pt]/[MT-2]: 0.5–0.95 mol/mol) in all reaction mixtures (Table 3), while only negligible Pt(II) binding to ZnFs was detected ([Pt]/[ZnF-1/-6]: <0.07 mol/mol; Table 3). Accordingly, direct determination of zinc-to-protein ratios in the recovered ZnF domain fractions revealed that no Pt(II)-dependent zinc release occurred in ZnFs ([Zn]/[ZnF]: 0.98–1.18 mol/mol) in agreement with Pt(II) preferential binding to MT-2. Pt(II) binding to Zn_7MT-2 thiolates results in concomitant stoichiometric zinc release[46] and thus the final Zn-to-MT ratios were extrapolated from the total metal quantification (zinc plus platinum), because protein determination concentration in platinated MTs could not be performed

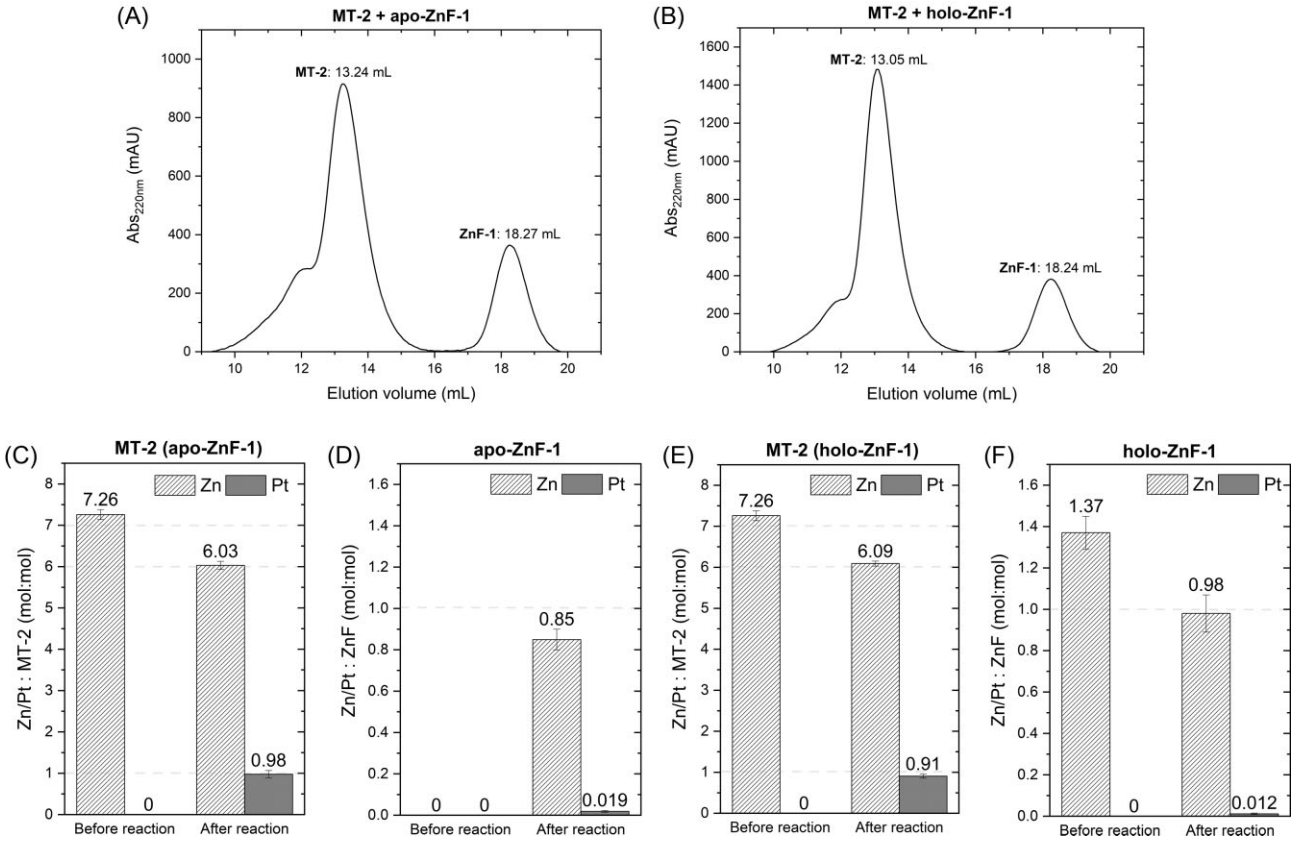

Fig. 3 Cisplatin competitive reaction between Zn_7MT-2 and apo-/holo-ZnF-1. (A) A mixture containing Zn_7MT-2, apo-ZnF-1, and cisplatin (1:1:1 molar ratio) was allowed to react for 120 h at 37°C before separating individual protein peaks by size exclusion chromatography on a Superdex 75 10/300 column. (B) A similar competitive reaction was performed between Zn_7MT-2, holo-ZnF-1, and cisplatin. After separation, the Zn- and Pt-concentrations of each individual protein-containing fraction were determined using ICP-MS in samples digested in HNO_3. Zn-/Pt-content of each peak after the chromatographic separation is presented as Zn/Pt: MT-2 or Zn/Pt: ZnF ratios (mol: mol): (C) MT-2 after reaction with apo-ZnF-1, (D) ZnF-1 upon reaction of apo-ZnF-1 with Zn_7MT-2, (E) MT-2 after reaction with holo-ZnF-1, and (F) ZnF-1 upon reaction of holo-ZnF-1 with Zn_7MT-2.

Table 3. Metal-to-protein ratios (mol/mol) before and after the cisplatin competitive reaction between Zn_7MT-2 and holo-ZnF-1/-6

Reaction mixture	[Zn]/[MT-2] before reaction	[Zn]/[ZnF-x] before reaction	[Zn]/[MT-2] after reaction	[Pt]/[MT-2] after reaction	[Zn]/[ZnF-x] after reaction	[Pt]/[ZnF-x] after reaction
Zn_7MT-2 + holo-ZnF-1 + cisplatin	7.26 ± 0.12	1.37 ± 0.08	6.09 ± 0.06	0.91 ± 0.05	0.98 ± 0.09	0.012 ± 0.004
Zn_7MT-2 + holo-ZnF-2 + cisplatin	7.26 ± 0.12	1.08 ± 0.08	6.51 ± 0.08	0.50 ± 0.07	1.03 ± 0.09	0.042 ± 0.030
Zn_7MT-2 + holo-ZnF-3 + cisplatin	7.26 ± 0.12	1.25 ± 0.23	6.05 ± 0.06	0.95 ± 0.06	0.99 ± 0.04	0.0056 ± 0.0003
Zn_7MT-2 + holo-ZnF-4 + cisplatin	7.26 ± 0.12	0.91 ± 0.06	6.45 ± 0.08	0.55 ± 0.06	1.00 ± 0.03	0.028 ± 0.002
Zn_7MT-2 + holo-ZnF-5 + cisplatin	7.26 ± 0.12	0.91 ± 0.02	6.35 ± 0.20	0.65 ± 0.03	1.18 ± 0.03	0.070 ± 0.028
Zn_7MT-2 + holo-ZnF-6 + cisplatin	7.26 ± 0.12	1.19 ± 0.04	6.464 ± 0.003	0.536 ± 0.002	0.98 ± 0.02	0.009 ± 0.001

Table 4. Metal-to-protein ratios (mol/mol) before and after the cisplatin competitive reaction between Zn_7MT-2 and apo-ZnF-1/-6

Reaction mixture	[Zn]/[MT-2] before reaction	[Zn]/[ZnF-x] before reaction	[Zn]/[MT-2] after reaction	[Pt]/[MT-2] after reaction	[Zn]/[ZnF-x] after reaction	[Pt]/[ZnF-x] after reaction
Zn_7MT-2 + apo-ZnF-1 + cisplatin	7.26 ± 0.12	-	6.03 ± 0.10	0.98 ± 0.09	0.85 ± 0.05	0.019 ± 0.005
Zn_7MT-2 + apo-ZnF-2 + cisplatin	7.26 ± 0.12	-	6.15 ± 0.15	0.93 ± 0.03	0.74 ± 0.06	0.067 ± 0.031
Zn_7MT-2 + apo-ZnF-3 + cisplatin	7.26 ± 0.12	-	6.17 ± 0.08	0.83 ± 0.07	0.79 ± 0.08	0.015 ± 0.001
Zn_7MT-2 + apo-ZnF-4 + cisplatin	7.26 ± 0.12	-	6.15 ± 0.09	0.85 ± 0.08	0.76 ± 0.05	0.027 ± 0.008
Zn_7MT-2 + apo-ZnF-5 + cisplatin	7.26 ± 0.12	-	6.34 ± 0.01	0.66 ± 0.01	0.74 ± 0.01	0.014 ± 0.007
Zn_7MT-2 + apo-ZnF-6 + cisplatin	7.26 ± 0.12	-	6.34 ± 0.03	0.73 ± 0.03	0.84 ± 0.01	0.008 ± 0.003

by standard photometric methods due to interference with CysS-Pt(II) LMCT contributions. We subsequently investigated the competitive reaction of apo-ZnFs versus MT-2. Reactivity of zinc metal binding sites in apo-ZnFs is expected to be higher than the corresponding holo-ZnFs. We thus investigated whether preferential Pt(II) binding to MTF-1 apo ZnFs would be favored over the cisplatin reaction with fully metallated Zn_7MT-2. Metal quantification analysis upon MT-2 and Zn fingers separation in the reaction mixtures revealed that, also in the case of apo-ZnFs, cisplatin preferentially reacts with Zn_7MT-2 resulting in MT-2 platination approaching stoichiometric ratios ([Pt]/[MT-2]: 0.66–0.98 mol/mol). Accordingly, no significant Pt(II) binding to apo-ZnFs was detected ([Pt]/[ZnF-1/-6]: <0.07 mol/mol; Table 4). As MT-2 platination results in concomitant Zn^{2+} release, we quantified the Zn content in ZnF samples at the end of the reaction. The results revealed close to stoichiometric Zn(II) reconstitution of all apo ZnFs ([Zn]/[ZnF-1/-6]: 0.74–0.85 mol/mol; Table 4). These results indicate that Pt(II) binding to MTs appears to be thermodynamically and/or kinetically favored over binding to MTF-1 ZnFs, and that MT-2 can act as a sink for cisplatin inactivation. In addition, the apparent transfer of released zinc from MTs to MTF-1 ZnF could potentially lead to MTF-1 activation upon zinc binding to its ZnFs.

Zinc binding affinities in ZnF-1/-6 *versus* Zn_7MT-2

The conducted experiments did not address on whether the stoichiometric zinc transfer between Zn_7MT-2 and MTF-1 apo ZnFs takes place prior to Pt(II) reaction with Zn_7MT-2 to generate partially depleted Zn_xMT-2, or whether the zinc transfer is cisplatin-dependent and consequent to cisplatin- mediated zinc release from MT-2. To address this question, comparative average Zn(II) dissociation constants were determined for Zn^{2+}-ZnF-1/-6 and Zn_7MT-2.

We proceeded in determining the overall average Zn(II) binding affinities using the chromogenic zinc chelator 4-(2-pyridylazo)resorcinol (PAR). PAR forms a stable 2:1 complex with Zn(II), $ZnH_x(PAR)_2$, with a high molar absorption coefficient (ε_{492} = 71500 M^{-1} cm^{-1}) that allow for the detection of low Zn(II) concentrations.[84] Zn^{2+}-ZnF-1/-6 (10 μM) and Zn_7MT-2 (10 μM) samples were reacted with 20 μM PAR for 24 h in anaerobic atmosphere and the absorbance at 492 nm was later measured to determine the concentration of $ZnH_x(PAR)_2$. The average Zn(II) dissociation constants were subsequently calculated using the effective dissociation constant of $ZnH_x(PAR)_2$ at pH 7.4 (K_d^{eff} = 7.08 × 10^{-13} M^2).[81]

Table 5. Zn^{2+} dissociation constants (K_D) of ZnF-x-Zn^{2+} (x = 1–6), *h*MTF-1-*zf*-domain and Zn_7MT-2 samples determined from competition reactions with PAR at pH 7.4 in anaerobic atmosphere

Protein/peptide-Zn^{2+}	K_D (M)
ZnF-1-Zn^{2+}	1.17 (± 0.50) × 10^{-9}
ZnF-2-Zn^{2+}	1.26 (± 0.28) × 10^{-10}
ZnF-3-Zn^{2+}	5.20 (± 1.50) × 10^{-10}
ZnF-4-Zn^{2+}	4.19 (± 0.95) × 10^{-10}
ZnF-5-Zn^{2+}	1.55 (± 0.68) × 10^{-10}
ZnF-6-Zn^{2+}	5.21 (± 0.54) × 10^{-10}
*h*MTF-1-*zf*-domain	8.93 (± 2.44) × 10^{-10}
Zn_7MT-2	4.72 (± 1.91) × 10^{-11}[a]

The values were calculated using the molar absorption coefficient at 492 nm (ε_{492} = 71500 M^{-1} cm^{-1}) and the effective dissociation constant (K_d^{eff} = 7.08 × 10^{-13} M^2) of $ZnH_x(PAR)_2$. The Zn_7MT-2 and *h*MTF-1-*zf*-domain values correspond to the average K_D for all zinc binding sites. Values are reported as average of technical replicates ± standard deviation (n = 3).
[a]3.06 (± 0.12) × 10^{-11} reported in Calvo *et al.* (2018).

The calculated Zn^{2+} dissociation constants (Table 5) for the isolated ZnFs ZnF-1/-6 confirmed an overall affinity falling in the nano- to picomolar range and that zinc affinity for the different ZnF varies over less than one order of magnitude across the series.

Despite the apparent relative order of affinity for the different ZnFs determined here (ZnF-2 ~ ZnF-5 > ZnF-3 ~ ZnF-4 ~ ZnF-6 > ZnF-1) is slightly different that the ones obtained upon Co^{2+} titration of peptides corresponding to mouse MTF-1 ZnFs (ZnF-2 ~ ZnF-3 ~ ZnF-4 > ZnF-1 ~ ZnF-5 ~ ZnF-6), which might be

related to small differences in peptide sequences, experimental design, and different metals investigated (Co^{2+} versus direct Zn^{2+} affinity determination), the results are consistent with none of the Cys_2His_2 ZnF domains of MTF1 having a dramatically lower metal ion affinity compared to the others.[59,63] In addition, the determined values are in agreement with the investigation on fragments of mMTF-1 including all six ZnF domains, suggesting that the zinc(II) affinities of the mMTF-1 peptides are in the sub-nanomolar range.[59]

The corresponding average zinc dissociation constant in Zn_7MT-2 ($K_D \sim 4 \times 10^{-11}$ M) indicated that Zn_7MT-2 possesses an average zinc binding affinity that is one to two orders of magnitude higher that the ones observed for each of the ZnFs peptide investigated in this study (ZnF-1/-6). It should be noted that the seven Zn(II) ions appear to possess different affinities when bound to MT-2, with the presence for four higher affinity sites ($K_D \sim 10^{-12}$ M) and three weaker sites (two sites with Kd $\sim 10^{-11}$–10^{-10} M, and one site with Kd $\sim 10^{-8}$ M, respectively), likely located in the β-domain.[96] Recent work by Krężel and coworkers on MT-2 Zn(II) metalation elegantly demonstrated that the α-domain $Zn(II)_4$-thiolate cluster is formed sequentially in the first stages, followed by the sequential formation of the β-domain $Zn(II)_3$-thiolate cluster, although both processes partially overlap. The study also revealed that the weakest Zn(II) ions associates with the β-domain indicating that the three weaker sites are located in the N-terminal β-domain three-metal cluster.[97]

Based on these considerations and the determined K_D values, we thus performed control experiments upon coincubation of Zn_7MT-2 with apo-ZnFs under the same conditions utilized in competition reactions with cisplatin, followed by chromatographic separation and zinc-content quantification to analyze whether cisplatin-independent zinc transfer can take place. The results indicate that stoichiometric Zn(II) transfer from Zn_7MT-2 to ZnFs does not take place in absence of cisplatin (Supplementary Fig. 7). Thus, despite the presence of a lower affinity zinc site in Zn_7MT-2 which could potentially result in substoichiometric Zn(II) transfer to ZnFs, full ZnFs reconstitution requires cisplatin-mediated zinc displacement in MT-2. Thus, kinetic bias contributions might be responsible for the absence of Zn(II) transfer. Overall, these investigations support that MT-2 can compete for zinc binding to MTF-1 and that stoichiometric zinc transfer from Zn_7MT-2 to apo-MTF-1 (or partially metallated MTF-1), resulting in its activation, might not be kinetically (and to a certain extent thermodynamically) favorable if fully or partially metallated Zn_xMT-2 is present. These conclusions were also confirmed in an EMSA in which coincubation of Zn_7MT-2 with zinc-depleted *h*MTF-1-*zf*-domain did not result in MTF-1 activation and binding to a double-stranded oligonucleotide containing the MRE consensus sequence that is recognized by MTF-1 (vide infra).

Overall, the results obtained in the competition experiments are also supported by the apparent zinc binding affinity and metal transfer determinations, supporting the observed preferential reactivity of cisplatin towards MT-2 and possible zinc transfer from MT-2 to MTF-1 ZnFs.

Kinetics of cisplatin binding to apo- and holo-ZnF-1/-6 versus Zn_7MT-2

Based on previous investigations, ligand replacement rates on Pt(II) complexes by thiols and thioether ligands can be faster than for nitrogens on heteroaromatic groups, and Pt(II)–sulfur interactions can be kinetically preferred.[76] We thus investigated whether cisplatin binding to MT-2 is kinetically favored compared to MTF-1 ZnFs.

To investigate the comparative reaction kinetics and estimate the relative apparent reaction velocities, the time courses of Pt(II) binding to Zn_7MT-2 thiolates versus apo- and holo-ZnF-1/-6 were recorded under conditions identical to the ones utilized for the competitive reaction studies described above (Fig. 4). The formation of CysS-Pt(II) bonds was followed by absorption spectroscopy at 285 nm as a function of time in anaerobic atmosphere, in gas-tight sealed cuvettes. The reported absorption spectrum of platinated proteins containing sulfur ligands, as exemplified by Pt(II)-MT species, is characterized by broad, unresolved absorption bands with an extensive shoulder at 250 nm and tailing up to 400 nm. These absorption features arise from two $L\pi \rightarrow M\sigma^*$ (i.e. CysS-Pt(II)) LMCT transitions close in energy.[51] Since at ∼250 nm the contribution of CysS-Zn(II) LMCT absorption tailing overlaps with CysS-Pt(II) LMCT transitions, the change in absorption at 285 nm was used to derive the number of CysS-Pt(II) bonds participating in the Pt(II) coordination after the 120-h reaction. The use of this wavelength is supported by previous studies demonstrating a linear dependence of the absorbance contributions versus the number of Pt(II) bound at ∼280 nm, but not at lower wavelengths.[51]

In the reaction of Zn_7MT-2 with cisplatin, it has been demonstrated that all ligands are replaced by cysteine thiolates and an average extinction coefficient for each CysS-Pt(II) bond was estimated to be $\varepsilon_{285} \sim 2850$ M^{-1} cm^{-1}.[46] We thus utilized $\varepsilon_{285} = 2850$ M^{-1} cm^{-1} for the relative quantification of CysS-Pt(II) in MT-2 and ZnF-1/-6 after the 120-h reaction. It should be noted that, small variations (∼10%) of this extinction coefficients are expected to occur as a function of the ligand sets that are present on the Pt(II) binding sites. Analysis of the evolution of the kinetic traces indicates that cisplatin binding to Zn_7MT-2, as well as ZnFs, are multistep processes that result in multiphasic kinetic traces (Fig. 4). As the detailed mechanism of the Pt(II) binding processes cannot be derived from the kinetic traces collected in this work, we limited to calculate the relative number of CysS-Pt(II) bonds formed per protein per minute, from the absorption at 285 nm obtained in the first part of the reaction (5 h, Table 6). The results indicate that, regardless of the apparent differences in the kinetic profiles, likely reflecting differences in the platination mechanism of MT-2 versus ZnFs, the overall apparent kinetics of the Pt(II)–sulfur bond formation in Zn_7MT-2 is at least one order of magnitude faster than in apo- and holo-ZnFs. Moreover, while the calculation of the formed Pt(II)–sulfur bonds from the absorbance at 285 nm after 120 h is consistent with the replacement of all cisplatin ligands in MT-2 to form Cys_4-Pt(II) complexes, in apo- and holo-ZnFs no full substitution by both Cys thiolates of the Cys_2His_2 motif was observed, suggesting that no stoichiometric Cys_2His_2-Pt(II) complexes were formed in the course of the reaction (Table 6).[46] Nevertheless, these data indicate that the reactivity of different ZnFs towards cisplatin varies across the series and that ZnF-6 appears to be the most reactive ZnF domain, which is also in line with previous alkylation studies and the proposed model in which ZnF-6 might represent one of the sensing ZnFs in MTF-1.[93] The observed differences in reaction rates might also underlie structural differences existing across the MTF-1 ZnFs series that remains to be elucidated.

Taken together, our investigations suggest that cisplatin binding to MT-2 is favored when compared to MTF-1 ZnFs. Despite we cannot unambiguously dissect kinetic and thermodynamic contributions to this reactivity bias, we speculate that both aspects might be important for the preferential cisplatin reactivity

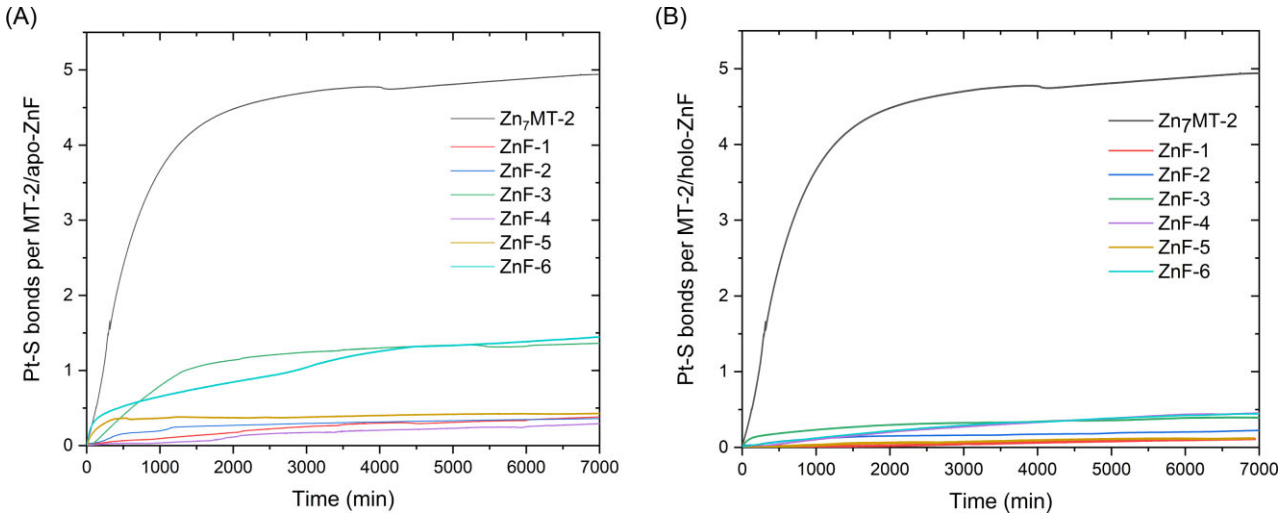

Fig. 4 Cisplatin binding kinetics upon reaction with Zn_7MT-2 and the individual apo-/holo ZnFs. Complex formation as a function of time was monitored by UV-Vis electronic absorption spectroscopy via absorption changes at 285 nm upon reacting cisplatin (20 μM) with Zn_7MT-2 (20 μM), with each apo-zinc finger peptides (A: apo-ZnF-1/-6), or holo-zinc-fingers (B: holo-ZnF-1/-6). Kinetic plots (as shown) were normalized to the number of Pt(II)-S bonds formed in each protein during reaction, using $\varepsilon_{285\ nm}$ of 2850 M^{-1} cm^{-1} per Pt(II)-S bond.[46] All reactions were carried out in 10 mM HEPES/HCl pH = 7.4, 100 mM $NaClO_4$ for 120 h at 37°C.

Table 6. CysS-Pt(II) bond formation upon reaction between cisplatin and Zn_7MT-2, apo-ZnF-1/-6, and holo-ZnF-1/-6

Protein/peptide	Pt-S bonds protein^{-1} min^{-1}	Pt-S bonds protein^{-1} at 120 h
Zn_7MT-2	(4.01 ± 1.31) × 10^{-3}	4.87 ± 0.14
apo-ZnF-1	(2.31 ± 0.60) × 10^{-4}	0.43 ± 0.18
apo-ZnF-2	(2.89 ± 0.29) × 10^{-4}	0.35 ± 0.01
apo-ZnF-3	(5.76 ± 1.31) × 10^{-4}	1.32 ± 0.03
apo-ZnF-4	(0.78 ± 0.32) × 10^{-4}	0.39 ± 0.07
apo-ZnF-5	(1.18 ± 0.69) × 10^{-3}	0.44 ± 0.01
apo-ZnF-6	(1.50 ± 0.02) × 10^{-3}	1.48 ± 0.02
holo-ZnF-1	(5.50 ± 1.92) × 10^{-5}	0.15 ± 0.05
holo-ZnF-2	(1.47 ± 0.22) × 10^{-5}	0.15 ± 0.06
holo-ZnF-3	(4.80 ± 0.51) × 10^{-4}	0.57 ± 0.15
holo-ZnF-4	(1.43 ± 0.58) × 10^{-4}	0.46 ± 0.01
holo-ZnF-5	(3.08 ± 1.65) × 10^{-5}	0.13 ± 0.01
holo-ZnF-6	(6.48 ± 1.41) × 10^{-4}	0.71 ± 0.18

Number Pt(II)-S bonds formed in the first 300 min of reaction and after 120-h incubation at 37°C were determined by changes in the absorption at 285 nm.

towards MT-2. This can be correlated to the effective kinetic *trans*-labilization of N-donors (NH_3 in cisplatin) located in *trans* position to the sulfur ligands, which accounts for the generation of Cys_4-Pt(II) complexes in MT-2 formed upon the reaction with cisplatin. Although the initial CysS-Pt(II) bond formation in MT-2 is a rather slow process, the subsequent ligand replacement is faster because of the *trans* effect, and also favored because all four Cys ligands are structurally constrained in close proximity within the targeted Zn(II)-cluster in MT-2. While *trans*-labilization of ligands in *trans* position to Cys is expected to occur also in Cys_2His_2 sites, our data indicate that this effect is less pronounced in ZnFs because the NH_3 replacement in *trans* position to Cys S ligands by His N ligands is likely less favorable than the Pt(II)–sulfur bond formation in MT-2. Kinetically disfavored cisplatin binding to the ZnFs might also be due to steric reasons as ZnFs feature secondary structural elements that might render coordination of a sterically more demanding Pt(II) complex more difficult. In agreement, the observed differences in platination rates in ZnFs (e.g. ZnF-3 and ZnF-6 showing faster platination but forming only one Pt(II)–sulfur bond) suggest potential contributions of steric restrictions in controlling reactivity towards cisplatin and potential structural differences in different ZnFs during binding. In addition, the thermodynamic stability of Cys_4-Pt(II) sites might overcome the overall stability of Pt(II) complexes formed in Cys2His2 sites that would require a distortion of their metal binding site for full Pt(II) coordination by protein ligands.

Competitive reaction of cisplatin towards the six ZnF domain of human MTF-1 (*h*MTF-1-*zf*-domain) versus Zn_7MT-2

The overall zinc binding properties (affinity and reactivity) of each ZnF appear to be partially tuned when the fingers are present in the context of the entire six ZnF domain of MTF-1.[59,93] Analysis of the cobalt binding affinity of each domain in the context of mouse MTF-1 six ZnF domain was demonstrated to be slightly increased when compared to the single domain peptides.[59] Moreover, the affinities of some of the fingers were more affected than others, suggesting possible modulation of the relative zinc binding affinity and reactivity properties by the presence of interfinger linkers and potential interfinger interactions.[59] In addition, the reactivity of cysteines in *h*MTF-1-ZnF domain in response to pulsed alkylation was found to follow the order ZnF-5 > ZnF-6 ≫ ZnF-1 > ZnF-2 ≈ ZnF-3 ≈ ZnF-4, further corroborating modulation of cysteine reactivity in Cys_2His_2 sites in the context of multidomain ZnF constructs.[93]

The preferential cisplatin reactivity towards MT-2 observed with isolated MTF-1 ZnFs was thus investigated in the context of the entire human MTF-1 ZnF domain. We developed a strategy to recombinantly express the *h*MTF-1-*zf*-domain in *E. coli* and purify it by affinity chromatography in its Zn^{2+}-bound form through an N-terminal STREP-tag in the presence of excess Zn^{2+} (Supplementary Fig. 8). The protein was purified at >95% purity, and zinc-to-protein (5.50 ± 0.23 mol/mol) and cysteine-to-protein ratios (10.69 ± 0.66 mol/mol) were consistent with a successful zinc reconstitution of the purified *h*MTF-1-*zf*-domain. We determined the average zinc binding affinity of the

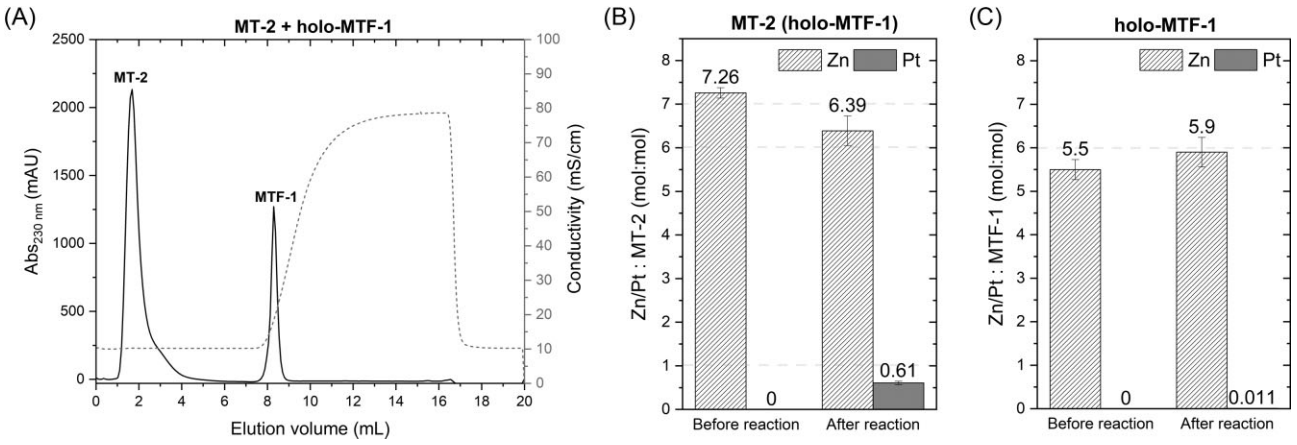

Fig. 5 Cisplatin competitive reaction between Zn_7MT-2 and holo-MTF-1-*zf*-domain. (A) A mixture containing Zn_7MT-2, holo-MTF-1, and cisplatin (40 μM; 1:1:1 molar ratio) in 10 mM HEPES/HCl pH = 7.4, 100 mM $NaClO_4$, was allowed to react for 120 h at 37°C before separating individual protein peaks by anion exchange chromatography using a HiTrap Q column. After separation, the Zn- and Pt-concentrations of each individual protein-containing fraction were determined using ICP-MS in samples digested in HNO_3. Zn-/Pt-content of each peak after the chromatographic separation is presented as Zn/Pt: MT-2 or Zn/Pt: MTF-1-*zf*-domain ratios (mol: mol): (B) MT-2 and (c) MTF-1-*zf*-domain.

holo-*h*MTF-1-*zf*-domain with the chromogenic zinc chelator 4-(2-pyridylazo)resorcinol (PAR), following the same procedure utilized with isolated ZnF peptides. The obtained average zinc dissociation constant ($K_D = 8.93 \pm 2.44 \times 10^{-10}$ M, Table 5), which represents the average binding affinity of all ZnFs in the *h*MTF-1-*zf*-domain, suggests that despite possible changes in the zinc affinities in each ZnF in context of the entire domain might exist, these changes should not affect the preferential favorable reactivity of cisplatin towards MT-2 as observed for isolated ZnFs.

To verify this hypothesis, cisplatin competition reactions in the presence of competing equimolar concentrations of Zn_7MT-2 and Zn_6-*h*MTF-1-*zf*-domain were conducted in anaerobic atmosphere as described above. Reaction mixtures were incubated in 10 mM HEPES/HCl pH 7.4, 100 mM $NaClO_4$ at 37°C, in absence of light, for 120 h. Subsequently, reaction mixtures were separated by ion exchange chromatography (Fig. 5A) and the fractions containing MT-2 and *h*MTF-1-*zf*-domain were collected for metal quantification (a control chromatogram of the mixture in absence of cisplatin is presented in Supplementary Fig. 9).

Analysis of Pt-to-protein ratios at the end of the reaction revealed preferential binding to Zn_7MT-2 ([Pt]/[MT-2]: 0.61 ± 0.04 mol/mol) (Fig. 5B), while negligible Pt(II) binding to Zn_6-*h*MTF-1-*zf*-domain was detected ([Pt]/[*h*MTF-1-*zf*-domain]: 0.011 ± 0.004 mol/mol; Fig. 5C).

Accordingly, with the preferential cisplatin reaction towards MT-2, zinc-to-protein ratio determinations confirmed zinc release from MT-2 ([Zn]/[MT-2]: 6.39 ± 0.34 mol/mol; Fig. 5B) but not from Zn_6-*h*MTF-1-*zf*-domain ([Zn]/[*h*MTF-1-*zf*-domain]: 5.90 ± 0.34 mol/mol; Fig. 5C).

These results further confirm that, while modulation of the reactivity of zinc centers in each finger in the context of the *h*MTF-1-*zf*-domain might occur, cisplatin reacts more efficiently with MT-2 Cys_4 sites than Cys_2His_2 sites present in MTF-1. This further corroborates that the cisplatin reaction with Zn_7MT-2, leading to zinc release, might in turn result in MTF-1 activation upon zinc transfer to MTF-1.

It should be noted that we also attempted to characterize the reactivity of apo-*h*MTF-1-*zf*-domain. However, while the apo-*h*MTF-1-*zf*-domain could be successfully generated by treatment with EDTA and subsequent dialysis (Table 2), the generated apo-protein resulted to be extremely prone to aggregation and precipitation in the course of the 120-h reaction with cisplatin in the presence of MT-2, most likely due to the high susceptibility to misfolding and/or oxidation when Zn^{2+} is absent from all the ZnFs. Thus, detailed characterization of the reaction products was not possible in the case of the apo-*h*MTF-1-*zf*-domain.

*h*MTF-1-*zf*-domain activation via cisplatin-dependent Zn^{2+}-transfer from Zn_7MT-2 and DNA binding monitored by EMSA

The modality by which MTF-1 is activated by zinc remains still to be fully elucidated, but it has been postulated that full reconstitution of the Zn finger domain is necessary for MRE binding and the subsequent transcriptional activation of genes downstream of the MRE elements, such as MT-1/-2 genes.

A model suggesting that all MTF-1 Cys_2His_2 ZnF domains have an intrinsically low affinity for zinc and folding into an appropriate structure occurs only at high zinc concentrations was initially proposed but disputed by subsequent studies.[98] Subsequent investigations revealed that individual fingers of MTF-1 have different zinc affinities, and it was proposed that the MTF-1 ZnFs with higher affinity for zinc possess a structural role, while the fingers with lower zinc affinity binding sites act as metal sensors and thus regulate MTF-1 activation as a function of fluctuations in zinc cellular concentrations.[59,62,63,93,99–101] The reactivity of cysteines in *h*MTF-1-*zf*-domain towards pulsed alkylation followed the order ZnF-5 > ZnF-6 ≫ ZnF-1 > ZnF-2 ≈ ZnF-3 ≈ ZnF-4.[62,93,99] In addition, while binding of *h*MTF-1 to an MRE-containing double-stranded oligonucleotide decreased the fingers' reactivity towards alkylation, ZnF-5 and ZnF-6 were still the most reactive, while deletion of ZnF-1 led to poor MRE binding. Together with NMR studies on *h*MTF-1 constructs containing ZnF-4 through ZnF-6 showing exchange broadening of resonances at saturating zinc levels, a model in which domains 5 and 6 act as sensors controlling the zinc-induced MTF-1 activation and subsequent DNA binding was proposed.[62,99] Nevertheless, other studies determining the metal binding affinities via cobalt titration of the six Cys_2His_2 ZnF domains alone and in the context of MTF-1 revealed that the metal ion affinities of specific ZnFs are not dramatically lower than those observed for other ZnFs.[59] However, ZnF-1, ZnF-3, and ZnF-6 showed lower affinities in the context of a six ZnF protein

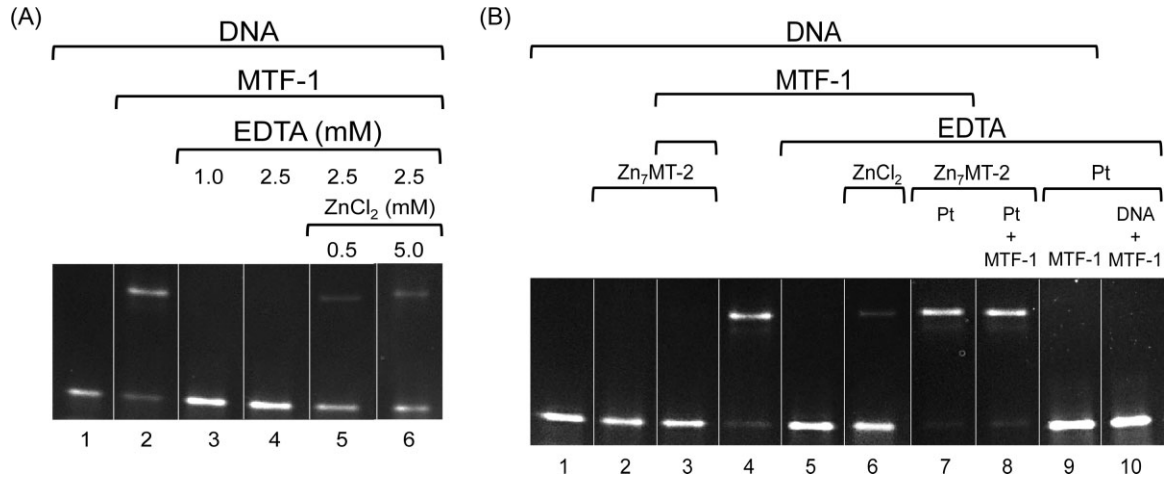

Fig. 6 Native electrophoretic mobility shift assays (EMSA) demostrating activation of MTF-1-*zf*-domain via cisplatin-dependent Zn^{2+} transfer from Zn_7MT-2. (A) Native EMSA gel for samples containing the MRE 6FAM-labeled double-stranded oligonucleotide (1 pmol; lane 1), the MRE oligonucleotide in the presence of Zn_6-MTF-1-*zf*-domain (10 μM; lane 2), the MRE oligonucleotide in the presence of Zn_6-MTF-1-*zf*-domain (10 μM) with increasing concentration of EDTA (1–2.5 mM; lanes 3 and 4), or the MRE oligonucleotide in the presence of Zn_6-MTF-1-*zf*-domain (10 μM), EDTA (2.5 mM) and supplemented with increasing Zn^{2+} concentrations (0.5–5.0 mM; lanes 5 and 6). (B) Native EMSA gel for samples containing the MRE 6FAM-labeled double-stranded oligonucleotide (1 pmol) alone (lane 1), in the presence of Zn_7MT-2 (0.5 mM) alone (lane 2), in the presence of Zn_6-MTF-1-*zf*-domain (10 μM) with EDTA (2.5 mM) upon incubation of MTF-1-*zf*-domain with Zn_7MT-2 (0.5 mM; lane 3), in the presence of Zn_6-MTF-1-*zf*-domain (10 μM) alone (lane 4), in the presence of Zn_6-MTF-1-*zf*-domain (10 μM) with EDTA (2.5 mM; lane 5), in the presence of Zn_6-MTF-1-*zf*-domain (10 μM) with EDTA (2.5 mM) supplemented with Zn^{2+} (0.5 mM; lane 6), in the presence of Zn_6-MTF-1-*zf*-domain (10 μM) with EDTA (2.5 mM) and the product of the reaction between Zn_7MT-2 (0.5 mM) and cisplatin (0.5 mM) (lane 7), or in the presence of Zn_6-MTF-1-*zf*-domain (10 μM) upon coincubation of the MTF-1-*zf*-domain with the product of the reaction between Zn_7MT-2 and cisplatin (0.5 mM) and adding EDTA (2.5 mM) prior to EMSA (lane 8). Crosslinking between DNA and MTF-1 in the presence of cisplatin was not observed when the oligonucleotide was incubated with EDTA (2.5 mM) and the product of the reaction between Zn_6-MTF-1-*zf*-domain (10 μM) and cisplatin (0.5 mM; lane 9), or when DNA was coincubated with Zn_6-MTF-1-*zf*-domain (10 μM) and cisplatin (0.5 mM) and EDTA (2.5 mM) was added prior to EMSA (lane 10).

fragment, leading to the suggestion that ZnF-1 and ZnF-6 act as sensor domains responsible for MTF-1 activation.[59] While the determination of the detailed mode of zinc sensing by MTF-1 is out of the scope of our investigation, there is a consensus that partially metallated *h*MTF-1 (or apo-MTF-1) requires full occupancy of their ZnFs to result in activation.

To investigate whether cisplatin-dependent zinc release from Zn_7MT-2 and transfer to MTF-1 results in MTF-1 activation and binding to MRE, we investigated via EMSA the recognition and binding of *h*MTF-1-*zf*-domain to a fluorescently labeled double-stranded oligonucleotide featuring the consensus MRE motif. Our initial test verifying the binding of MTF-1 to the designed oligonucleotide by EMSA showed that in comparison to the free oligonucleotide, the expected band shift could be detected with our recombinantly expressed Zn_6MTF-1-*zf*-domain, thus confirming the proper folding needed for MRE recognition and DNA binding (Fig. 6A, lanes 1 and 2). Coincubation of Zn_6MTF-1-*zf*-domain with increasing EDTA concentrations (Fig. 6A, lanes 3 and 4) revealed that the MRE binding is indeed zinc-dependent, thereby identifying experimental conditions for EDTA competition leading to abolishment of MTF-1 DNA binding. This effect could be reverted, and the DNA binding could be recovered upon external zinc supplementation of the samples treated with EDTA (Fig. 6A, lanes 5 and 6). Thus, we investigated whether, under the conditions in which the MTF-1 binding is abolished, the MTF-1-*zf*-domain could be reactivated via cisplatin-dependent zinc transfer from Zn_7MT-2. While coincubation of the labeled oligonucleotide with MTF-1-*zf*-domain resulted in a significant band shift (positive controls; Fig. 6B, lanes 1 and 4), no significant band shift was observed when MTF-1-*zf*-domain was treated with EDTA (2.5 mM) or when the oligonucleotide was mixed with Zn_7MT-2 (negative controls; Fig. 6B, lanes 2 and 5). However, MTF-1-*zf*-domain binding in the presence of EDTA could be restored in samples in which the MTF-1-*zf*-domain was mixed with the product of reaction between Zn_7MT-2 and cisplatin (120 h reaction; Fig. 6B, lane 7) or when MTF-1-*zf*-domain and Zn_7MT-2 were co-incubated with cisplatin for 120 h (Fig. 6B, lane 8). This binding could be restored in MTF-1 samples (in the presence of EDTA) that were externally supplemented with sufficient Zn^{2+} to re-metallate MTF-1 upon depletion by EDTA (Fig. 6B, lane 6), while coincubation with Zn_7MT-2 in absence of cisplatin did not result in DNA binding (Fig. 6B, lane 3). Moreover, cisplatin-mediated crosslinking between DNA and MTF-1 does not take place as no band shifts were seen in samples where the oligonucleotide were either mixed with the product of the reaction between MTF-1-*zf*-domain and cisplatin (Fig. 6B, lane 9), or when coincubated as a mixture for 120 h (Fig. 6B, lane 10).

Thus, our EMSA investigation confirmed that while zinc removal from fully zinc reconstituted MTF-1-*zf*-domain results in abolishment of MRE binding, the preferential reactivity of cisplatin towards Zn_7MT-2, leading to zinc release and transfer to MTF-1, can result in effective MTF-1-*zf*-domain reactivation and restore its ability to bind to the double-stranded oligonucleotide featuring the MRE sequence.

We cannot conclude on whether the zinc transfer involves the formation of transient complexes between MT-2 and MTF-1 or not. However, in the cellular context, in addition to MT expression in the cytosol, nuclear localization of MT-2 is observed in cancer cells that show resistance against cisplatin, suggesting that while competition reactions could hypothetically occur, the favorable reaction of cisplatin with MT-2 rather than MTF-1 ZnFs could be sufficient for acquisition of MT-mediated drug resistance. This preferential reactivity could underlie an increase in zinc levels necessary for Zn-dependent activation of MTF-1, regardless if a direct transfer via a ternary complex formation takes place.

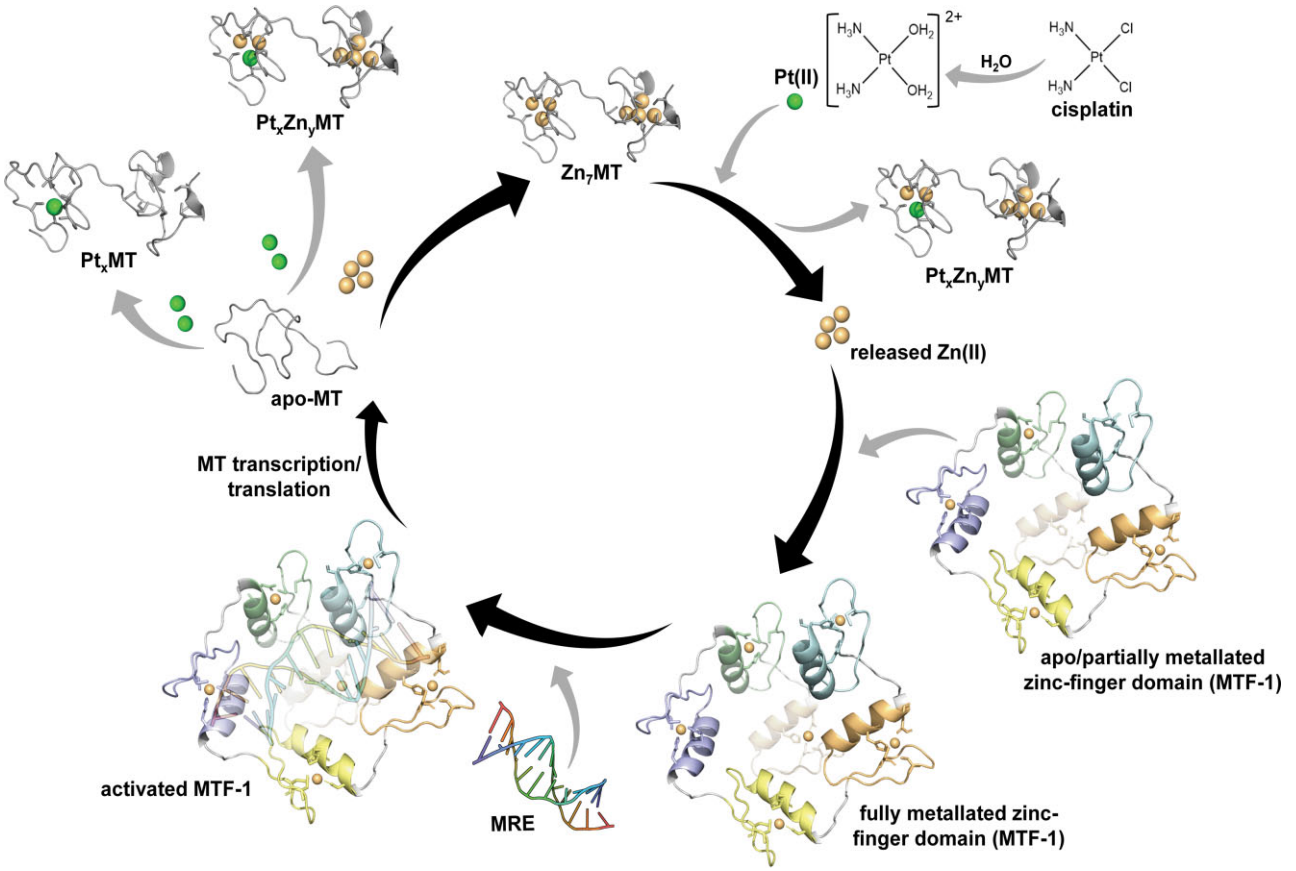

Fig. 7 Proposed scheme for the cisplatin-mediated activation of human MTF-1 via Zn release and transfer from MTs leading to drug resistance. As Zn(II) is released from Zn_7MT-2 upon its interaction with Pt(II), the apo/partially metallated zinc finger domain of MTF-1 is activated via zinc transfer and binding, generating the fully metallated MTF-1 and allowing its binding to metal-responsive elements (MRE) located in the promoter region of MT genes. MTF-1 mediated MT-gene transcription and translation results in elevated apo-MT-2 expression, which in turn can bind to Zn(II) and/or Pt(II) ions forming a variety of metallated MT adducts thus resulting in increased Pt(II) binding and sequestration and leading to cellular pre-target cisplatin resistance.

Conclusions

Overall, our investigations on the relative reactivity of Zn_7MT-2 and MTF-1 towards cisplatin allow us to formulate a possible model for cisplatin-dependent MT-mediated MTF-1 activation leading to acquired pre-target resistance (Fig. 7). Since MTs act as a first line of defense towards cellular metal toxicity and possess a higher reactivity towards cisplatin than MTF-1, in conditions of cellular cisplatin uptake, MTs can efficiently react with cisplatin leading to zinc displacement. This preferential reactivity, on one hand, results in MTF-1 protection from platination that would, in turn, cause its inactivation and reduce MT-1/-2 gene transcription and apo-MT expression. On the other, the cisplatin-dependent zinc release from MTs occurring in the nucleus of cancer cells (as well as in the cytoplasm) would result in increased free zinc levels and/or direct zinc transfer to apo/partially-metallated MTF-1, thus triggering MTF-1 activation. MTF-1 activation would lead to subsequent binding to the MRE sequences upstream of MT genes, triggering expression of apo-MTs. The increase in apo- and/or partially metallated MT cellular levels, triggered by cisplatin, could in turn lead to progressive increase the MT-mediated cellular ability to further scavenge cisplatin. Overall, our investigation provides the molecular basis to propose that the preferential reactivity of cisplatin towards MT-2 can underlie one of the potential mechanisms responsible for MT-mediated cisplatin resistance in which, upon cisplatin treatment, MTs act as a zinc reservoir for MTF-1 activation leading to MT overexpression, thereby increasing the cellular capacity towards Pt(II) complexes sequestration and reducing the desired cellular toxic effects of cisplatin treatment. As the investigations were based on *in vitro* analysis, additional work in cell cultures and *in vivo* will be required to quantify the impact of the observed MTs and MTF-1 reactivities and molecular processes on the MT-mediated anticancer Pt(II)-drug resistance. We envision that similar mechanisms can also occur with other Pt(II) complexes. Studies investigating the relative reactivity of a series of new generation *cis*- and *trans*-complexes towards MT-2 proposed that complexes showing lower reactivity towards MT and/or reduced ability to trigger zinc release as a function of their ligand nature and stereochemistry correlate with reduced development of resistance in cancer cells.[46] The model proposed here, based on our investigation, showing cisplatin-dependent MT-2-mediated MTF-1 activation, is consistent with the notion that the design of complexes that are less reactive towards MT can lead to a reduced ability to trigger MT-mediated pre-target acquired resistance.

Supplementary material

Supplementary data are available at *Metallomics* online.

Acknowledgements

The authors thank Manav Lund for assistance with experimental work.

Funding

The work was supported by the Robert A. Welch Foundation (AT-1935-20170325 and AT-2073-20210327 to G.M, and AT-1989-20190330 to J.J.G.), and by the National Institute of General Medical Sciences of the National Institutes of Health under Award Number R35GM128704 (to G.M.). The content is solely the responsibility of the authors and does not necessarily represent the official views of the National Institutes of Health.

Conflicts of interests

There are no conflicts of interest to declare.

Data availability

The data underlying this article will be shared on reasonable request to the corresponding author.

Note

This article is dedicated to the memory of Prof. Deborah Zamble, for her many seminal contributions to the field of bioinorganic chemistry and metallomics, including original work in the platinum drugs field. This research article is also dedicated to the memory of Prof. Milan Vašák, who contributed the hypothesis at the basis of this work, and for his continuous contributions to the metallothionein field.

References

1. D. Wang and S. J. Lippard, Cellular processing of platinum anticancer drugs, *Nat. Rev. Drug Discov*, 2005, 4 (4), 307–320.
2. B. Rosenberg, L. Vancamp and T. Krigas, Inhibition of cell division in *Escherichia coli* by electrolysis products from a platinum electrode, *Nature*, 1965, 205 (4972), 698–699.
3. B. Rosenberg, L. Vancamp, E. B. Grimley and A. J. Thomson, Inhibition of growth or cell division in Escherichia coli by different ionic species of platinium(IV) complexes, *J. Biol. Chem.*, 1967, 242 (6), 1347–1352.
4. B. Rosenberg, E. Renshaw, L. Vancamp, J. Hartwick and J. Drobnik, Platinum-induced filamentous growth in Escherichia coli, *J. Bacteriol.*, 1967, 93 (2), 716–721.
5. E. R. Jamieson and S. J. Lippard, Structure, recognition, and processing of cisplatin-DNA adducts, *Chem. Rev.*, 1999, 99 (9), 2467–2498.
6. C. A. Larson, B. G. Blair, R. Safaei and S. B. Howell, The role of the mammalian copper transporter 1 in the cellular accumulation of platinum-based drugs, *Mol. Pharmacol.*, 2009, 75 (2), 324–330.
7. G. Ciarimboli, Membrane transporters as mediators of cisplatin side-effects, *Anticancer Res.*, 2014, 34 (1b), 547–550.
8. D. B. Zamble and S. J. Lippard, Cisplatin and DNA repair in cancer chemotherapy, *Trends Biochem. Sci*, 1995, 20 (10), 435–439.
9. D. B. Zamble, D. Mu, J. T. Reardon, A. Sancar and S. J. Lippard, Repair of cisplatin—DNA adducts by the mammalian excision nuclease, *Biochemistry*, 1996, 35 (31), 10004–10013.
10. D. B. Zamble and S. J. Lippard, The response of cellular proteins to cisplatin-damaged DNA, In B. Lippert (ed) *Cisplatin: Chemistry and Biochemistry of a Leading Anticancer Drug*. Wiley-VCH: Zürich, 1999, 71–110.
11. G. Chu, Cellular responses to cisplatin. The roles of DNA-binding proteins and DNA repair, *J. Biol. Chem.*, 1994, 269 (2), 787–790.
12. Y. Kasherman, S. Sturup and D. Gibson, Is glutathione the major cellular target of cisplatin? A study of the interactions of cisplatin with cancer cell extracts, *J. Med. Chem.*, 2009, 52 (14), 4319–4328.
13. M. Vašák and N. Romero-Isart *Encyclopedia of Inorganic Chemistry*, 2nd edn, In R. Bruce King (ed). J. Wiley & Sons Ltd, New York: 2005, 3208–3221.
14. M. Vašák and G. Meloni, Chemistry and biology of mammalian metallothioneins, *J. Biol. Inorg. Chem.*, 2011, 16 (7), 1067–1078.
15. W. Maret and A. Krężel, Cellular zinc and redox buffering capacity of metallothionein/thionein in health and disease, *Mol. Med.*, 2007, 13 (7-8), 371–375.
16. A. Krężel and W. Maret, The functions of metamorphic metallothioneins in zinc and copper metabolism, *Int. J. Mol. Sci.*, 2017, 18 (6), 1237.
17. A. Krężel and W. Maret, The bioinorganic chemistry of mammalian metallothioneins, *Chem. Rev.*, 2021, 121 (23), 14594–14648.
18. K. E. Duncan, T. T. Ngu, J. Chan, M. T. Salgado, M. E. Merrifield and M. J. Stillman, Peptide folding, metal-binding mechanisms, and binding site structures in metallothioneins, *Exp. Biol. Med.*, 2006, 231 (9), 1488–1499.
19. J. S. Scheller, G. W. Irvine and M. J. Stillman, Unravelling the mechanistic details of metal binding to mammalian metallothioneins from stoichiometric, kinetic, and binding affinity data, *Dalton Trans.*, 2018, 47 (11), 3613–3637.
20. A. Arseniev, P. Schultze, E. Wörgötter, W. Braun, G. Wagner, M. Vašák, J. H. R. Kägi and K. Wüthrich, Three-dimensional structure of rabbit liver Cd_7metallothionein-2a in aqueous solution determined by nuclear magnetic resonance, *J. Mol. Biol.*, 1988, 201 (3), 637–657.
21. P. Schultze, E. Wörgötter, W. Braun, G. Wagner, M. Vašák, J. H. Kägi and K. Wüthrich, Conformation of Cd_7-metallothionein-2 from rat liver in aqueous solution determined by nuclear magnetic resonance spectroscopy, *J. Mol. Biol.*, 1988, 203 (1), 251–268.
22. B. A. Messerle, A. Schäffer, M. Vašák, J. H. Kägi and K. Wüthrich, Three-dimensional structure of human [$^{113}Cd_7$]metallothionein-2 in solution determined by nuclear magnetic resonance spectroscopy, *J. Mol. Biol.*, 1990, 214 (3), 765–779.
23. B. A. Messerle, A. Schäffer, M. Vašák, J. H. Kägi and K. Wüthrich, Comparison of the solution conformations of human [Zn7]-metallothionein-2 and [Cd7]-metallothionein-2 using nuclear magnetic resonance spectroscopy, *J. Mol. Biol.*, 1992, 225 (2), 433–443.
24. W. Braun, M. Vašák, A. H. Robbins, C. D. Stout, G. Wagner, J. H. Kägi and K. Wüthrich, Comparison of the NMR solution structure and the x-ray crystal structure of rat metallothionein-2, *Proc. Natl. Acad. Sci. U. S. A.*, 1992, 89 (21), 10124–10128.
25. W. Maret, Oxidative metal release from metallothionein via zinc-thiol/disulfide interchange, *Proc. Natl. Acad. Sci. USA*, 1994, 91 (1), 237–241.
26. E. Artells, O. Palacios, M. Capdevila and S. Atrian, Mammalian MT1 and MT2 metallothioneins differ in their metal binding abilities, *Metallomics*, 2013, 5 (10), 1397–1410.
27. E. Artells, O. Palacios, M. Capdevila and S. Atrian, In vivo-folded metal-metallothionein 3 complexes reveal the Cu-thionein rather than Zn-thionein character of this brain-specific mammalian metallothionein, *FEBS J.*, 2014, 281 (6), 1659–1678.
28. O. Palacios, S. Atrian and M. Capdevila, Zn- and Cu-thioneins: a functional classification for metallothioneins? *J. Biol. Inorg. Chem.*, 2011, 16 (7), 991–1009.

29. J. S. Calvo, V. M. Lopez and G. Meloni, Non-coordinative metal selectivity bias in human metallothioneins metal-thiolate clusters, *Metallomics*, 2018, 10 (12), 1777–1791.
30. P. Dziegiel, B. Pula, C. Kobierzycki, M. Stasiolek and M. Podhorska-Okolow, Metallothioneins in normal and cancer cells, *Adv. Anat. Embryol. Cell. Biol.*, 2016, 218, 1–117.
31. M. D. Apostolova, I. A. Ivanova and M. G. Cherian, Signal transduction pathways, and nuclear translocation of zinc and metallothionein during differentiation of myoblasts, *Biochem. Cell. Biol.*, 2000, 78 (1), 27–37.
32. B. Werynska, B. Pula, B. Muszczynska-Bernhard, A. Gomulkiewicz, A. Piotrowska, R. Prus, M. Podhorska-Okolow, R. Jankowska and P. Dziegiel, Metallothionein 1F and 2A overexpression predicts poor outcome of non-small cell lung cancer patients, *Exp. Mol. Pathol.*, 2013, 94 (1), 301–308.
33. M. A. Skowron, M. Melnikova, J. G. H. van Roermund, A. Romano, P. Albers, J. Thomale, W. A. Schulz, G. Niegisch and M. J. Hoffmann, Multifaceted mechanisms of cisplatin resistance in long-term treated urothelial carcinoma cell lines, *Int. J. Mol. Sci.*, 2018, 19 (2), 590.
34. P. Surowiak, V. Materna, A. Maciejczyk, M. Pudelko, E. Markwitz, M. Spaczynski, M. Dietel, M. Zabel and H. Lage, Nuclear metallothionein expression correlates with cisplatin resistance of ovarian cancer cells and poor clinical outcome, *Virchows. Arch.*, 2007, 450 (3), 279–285.
35. J. Gumulec, M. Raudenska, V. Adam, R. Kizek and M. Masarik, Metallothionein - immunohistochemical cancer biomarker: a meta-analysis, *PLoS One*, 2014, 9 (1), e85346.
36. M. Shanker, D. Willcutts, J. A. Roth and R. Ramesh, Drug resistance in lung cancer, *Lung Cancer*, 2010, 1, 23–36.
37. T. Eckschlager, V. Adam, J. Hrabeta, K. Figova and R. Kizek, Metallothioneins and cancer, *Curr. Protein Pept. Sci.*, 2009, 10 (4), 360–375.
38. S. Krizkova, M. Ryvolova, J. Hrabeta, V. Adam, M. Stiborova, T. Eckschlager and R. Kizek, Metallothioneins and zinc in cancer diagnosis and therapy, *Drug Metab. Rev.*, 2012, 44 (4), 287–301.
39. S. Borchert, P. M. Suckrau, R. F. H. Walter, M. Wessolly, E. Mairinger, J. Steinborn, B. Hegedus, T. Hager, T. Herold, W. E. E. Eberhardt, J. Wohlschlaeger, C. Aigner, A. Bankfalvi, K. W. Schmid and F. D. Mairinger, Impact of metallothionein-knockdown on cisplatin resistance in malignant pleural mesothelioma, *Sci. Rep.*, 2020, 10 (1), 18677.
40. C. H. Choi, Y. J. Cha, C. S. An, K. J. Kim, K. C. Kim, S. P. Moon, Z. H. Lee and Y. D. Min, Molecular mechanisms of heptaplatin effective against cisplatin-resistant cancer cell lines: less involvement of metallothionein, *Cancer Cell Int.*, 2004, 4 (1), 6.
41. J. H. Lee, J. W. Chae, J. K. Kim, H. J. Kim, J. Y. Chung and Y. H. Kim, Inhibition of cisplatin-resistance by RNA interference targeting metallothionein using reducible oligo-peptoplex, *J. Control. Release*, 2015, 215, 82–90.
42. A. de Graeff, R. J. Slebos and S. Rodenhuis, Resistance to cisplatin and analogues: mechanisms and potential clinical implications, *Cancer Chemother. Pharmacol.*, 1988, 22 (4), 325–332.
43. Y. Saga, H. Hashimoto, S. Yachiku, T. Iwata and M. Tokumitsu, Reversal of acquired cisplatin resistance by modulation of metallothionein in transplanted murine tumors, *Int. J. Urol.*, 2004, 11 (6), 407–415.
44. T. Endo, M. Yoshikawa, M. Ebara, K. Kato, M. Sunaga, H. Fukuda, A. Hayasaka, F. Kondo, N. Sugiura and H. Saisho, Immunohistochemical metallothionein expression in hepatocellular carcinoma: Relation to tumor progression and chemoresistance to platinum agents, *J. Gastroenterol.*, 2004, 39 (12), 1196–1201.
45. S. L. Kelley, A. Basu, B. A. Teicher, M. P. Hacker, D. H. Hamer and J. S. Lazo, Overexpression of metallothionein confers resistance to anticancer drugs, *Science*, 1988, 241 (4874), 1813–1815.
46. M. Knipp, A. V. Karotki, S. Chesnov, G. Natile, P. J. Sadler, V. Brabec and M. Vašák, Reaction of Zn_7metallothionein with cis- and trans-$[Pt(N\text{-donor})_2Cl_2]$ anticancer complexes: trans-Pt(II) complexes retain their N-donor ligands, *J. Med. Chem.*, 2007, 50 (17), 4075–4086.
47. A. V. Karotki and M. Vašák, Interaction of metallothionein-2 with platinum-modified 5'-guanosine monophosphate and DNA, *Biochemistry*, 2008, 47 (41), 10961–10969.
48. A. V. Karotki and M. Vašák, Reaction of human metallothionein-3 with cisplatin and transplatin, *J. Biol. Inorg. Chem.*, 2009, 14 (7), 1129–1138.
49. A. Pattanaik, G. Bachowski, J. Laib, D. Lemkuil, C. F. Shaw 3rd, D. H. Petering, A. Hitchcock and L. Saryan, Properties of the reaction of cis-dichlorodiammineplatinum(II) with metallothionein, *J. Biol. Chem.*, 1992, 267 (23), 16121–16128.
50. J. Bongers, J. U. Bell and D. E. Richardson, Platinum(II) binding to metallothionein, *J. Inorg. Biochem.*, 1988, 34 (1), 55–62.
51. J. Bongers, J. U. Bell and D. E. Richardson, Platinum(II)-thiolate cluster formation in heptaplatinum metallothionein, *Inorg. Chem.*, 1991, 30 (3), 515–519.
52. D. L. Wong and M. J. Stillman, Capturing platinum in cisplatin: kinetic reactions with recombinant human apometallothionein 1a, *Metallomics*, 2018, 10 (5), 713–721.
53. A. Pattanaik, G. Bachowski, J. Laib, D. Lemkuil, C. F. Shaw, III, D. H. Petering, A. Hitchcock and L. Saryan, Properties of the reaction of *cis*-dichlorodiammineplatinum(II) with metallothionein, *J. Biol. Chem.*, 1992, 267 (23), 16121–16128.
54. A. T. Miles, G. M. Hawksworth, J. H. Beattie and V. Rodilla, Induction, regulation, degradation, and biological significance of mammalian metallothioneins, *Crit. Rev. Biochem. Mol. Biol.*, 2000, 35 (1), 35–70.
55. J. H. R. Kägi, Evolution, structure and chemical activity of class I metallothioneins: an overview. In K. T. Suzuki, N. Imura M. Kimura (eds), *Metallothionein III*, Birkhäuser Verlag: Basel, 1993, 29–56.
56. F. Radtke, R. Heuchel, O. Georgiev, M. Hergersberg, M. Gariglio, Z. Dembic and W. Schaffner, Cloned transcription factor MTF-1 activates the mouse metallothionein I promoter, *EMBO J.*, 1993, 12 (4), 1355–1362.
57. R. Heuchel, F. Radtke, O. Georgiev, G. Stark, M. Aguet and W. Schaffner, The transcription factor MTF-1 is essential for basal and heavy metal-induced metallothionein gene expression, *EMBO J.*, 1994, 13 (12), 2870–2875.
58. E. Brugnera, O. Georgiev, F. Radtke, R. Heuchel, E. Baker, G. R. Sutherland and W. Schaffner, Cloning, chromosomal mapping and characterization of the human metal-regulatory transcription factor MTF-1, *Nucleic Acids Res.*, 1994, 22 (15), 3167–3173.
59. A. L. Guerrerio and J. M. Berg, Metal ion affinities of the zinc finger domains of the metal responsive element-binding transcription factor-1 (MTF1), *Biochemistry*, 2004, 43 (18), 5437–5444.
60. P. Lichtlen and W. Schaffner, Putting its fingers on stressful situations: the heavy metal-regulatory transcription factor MTF-1, *Bioessays*, 2001, 23 (11), 1010–1017.
61. X. Chen, A. Agarwal and D. P. Giedroc, Structural and functional heterogeneity among the zinc fingers of human MRE-binding transcription factor-1, *Biochemistry*, 1998, 37 (32), 11152–11161.
62. D. P. Giedroc, X. Chen and J. L. Apuy, Metal response element (MRE)-binding transcription factor-1 (MTF-1): structure, function, and regulation, *Antioxid. Redox Signal*, 2001, 3 (4), 577–596.

63. B. M. Potter, L. S. Feng, P. Parasuram, V. A. Matskevich, J. A. Wilson, G. K. Andrews and J. H. Laity, The six zinc fingers of metal-responsive element binding transcription factor-1 form stable and quasi-ordered structures with relatively small differences in zinc affinities, *J. Biol. Chem.*, 2005, 280 (31), 28529–28540.
64. W. Lee, A. Haslinger, M. Karin and R. Tjian, Activation of transcription by two factors that bind promoter and enhancer sequences of the human metallothionein gene and SV40, *Nature*, 1987, 325 (6102), 368–372.
65. T. P. Dalton, D. Bittel and G. K. Andrews, Reversible activation of mouse metal response element-binding transcription factor 1 DNA binding involves zinc interaction with the zinc finger domain, *Mol. Cell. Biol.*, 1997, 17 (5), 2781–2789.
66. D. Bittel, T. Dalton, S. L. Samson, L. Gedamu and G. K. Andrews, The DNA binding activity of metal response element-binding transcription factor-1 is activated in vivo and in vitro by zinc, but not by other transition metals, *J. Biol. Chem.*, 1998, 273 (12), 7127–7133.
67. B. Zhang, O. Georgiev, M. Hagmann, C. Gunes, M. Cramer, P. Faller, M. Vašák and W. Schaffner, Activity of metal-responsive transcription factor 1 by toxic heavy metals and H2O2 in vitro is modulated by metallothionein, *Mol. Cell. Biol.*, 2003, 23 (23), 8471–8485.
68. K. Kluska, J. Adamczyk and A. Krężel, Metal binding properties, stability and reactivity of zinc fingers, *Coord. Chem. Rev.*, 2018, 367, 18–64.
69. S. M. Yuan, X. Ding, Y. Cui, K. J. Wei, Y. C. Zheng and Y. Z. Liu, Cisplatin preferentially binds to zinc finger proteins containing C3H1 or C4 motifs, *Eur. J. Inorg. Chem.*, 2017, 2017 (12), 1778–1784.
70. A. I. Anzellotti, Q. Liu, M. J. Bloemink, J. N. Scarsdale and N. Farrell, Targeting retroviral Zn finger-DNA interactions: a small-molecule approach using the electrophilic nature of trans-platinum-nucleobase compounds, *Chem. Biol.*, 2006, 13 (5), 539–548.
71. Z. F. Du, R. E. F. de Paiva, Y. Qu and N. Farrell, Tuning the reactivity of Sp1 zinc fingers with platinum complexes, *Dalton Trans.*, 2016, 45 (21), 8712–8716.
72. R. N. Bose, W. W. Yang and F. Evanics, Structural perturbation of a C4 zinc-finger module by cis-diamminedichloroplatinum(II): insights into the inhibition of transcription processes by the antitumor drug, *Inorg. Chim. Acta*, 2005, 358 (10), 2844–2854.
73. M. A. C. Morelli, A. Ostuni, P. L. Cristinziano, D. Tesauro and A. Bavoso, Interaction of cisplatin with a CCHC zinc finger motif, *J. Pept. Sci.*, 2013, 19 (4), 227–232.
74. R. K. Duman, R. T. Heath and R. N. Bose, Inhibition of Escherichia coli DNA polymerase-I by the anti-cancer drug cis-diaminedichloroplatinum(II): what roles do polymerases play in cis-platin-induced cytotoxicity?, *FEBS Lett.*, 1999, 455 (1-2), 49–54.
75. L. Maurmann and R. N. Bose, Unwinding of zinc finger domain of DNA polymerase I by cis-diamminedichloroplatinum(II), *Dalton Trans.*, 2010, 39 (34), 7968–7979.
76. J. Reedijk, Why does Cisplatin reach Guanine-N7 with competing S-donor ligands available in the cell?,*Chem. Rev.*, 1999, 99 (9), 2499–2510.
77. D. V. Deubel, Factors governing the kinetic competition of nitrogen and sulfur ligands in cisplatin binding to biological targets, *J. Am. Chem. Soc.*, 2004, 126 (19), 5999–6004.
78. J. K.-C. Lau and D. V. Deubel, Loss of ammine from platinum(II) complexes: Implications for cisplatin inactivation, storage, and resistance, *Chem. Eur. J.*, 2005, 11 (9), 2849–2855.
79. A. F. Holleman, E. Wiberg and N. Wiberg, *Inorganic Chemistry*, 101 ed., Walter de Gruyter: Berlin, New York, 2001.
80. P. Faller, D. W. Hasler, O. Zerbe, S. Klauser, D. R. Winge and M. Vašák, Evidence for a dynamic structure of human neuronal growth inhibitory factor and for major rearrangements of its metal-thiolate clusters, *Biochemistry*, 1999, 38 (31), 10158–10167.
81. M. Vašák, Metal removal and substitution in vertebrate and invertebrate metallothioneins, *Methods Enzymol.*, 1991, 205, 452–458.
82. G. Meloni, M. Knipp and M. Vašák, Detection of neuronal growth inhibitory factor (metallothionein-3) in polyacrylamide gels and by Western blot analysis, *J. Biochem. Bioph. Methods*, 2005, 64 (1), 76–81.
83. A. O. Pedersen and J. Jacobsen, Reactivity of the thiol group in human and bovine albumin at pH 3-9, as measured by exchange with 2,2'-dithiodipyridine, *Eur. J. Biochem.*, 1980, 106 (1), 291–295.
84. A. Kocyla, A. Pomorski and A. Krężel, Molar absorption coefficients and stability constants of metal complexes of 4-(2-pyridylazo)resorcinol (PAR): Revisiting common chelating probe for the study of metalloproteins, *J. Inorg. Biochem.*, 2015, 152, 82–92.
85. L. Trynda-Lemiesz, H. Kozlowski and B. K. Keppler, Effect of cis-, trans-diamminedichloroplatinum(II) and DBP on human serum albumin, *J. Inorg. Biochem.*, 1999, 77 (3-4), 141–146.
86. T. Peleg-Shulman and D. Gibson, Cisplatin-protein adducts are efficiently removed by glutathione but not by 5'-guanosine monophosphate, *J. Am. Chem. Soc.*, 2001, 123 (13), 3171–3172.
87. T. Peleg-Shulman and D. Gibson, Interactions of cisplatin and transplatin with proteins. Comparison of binding kinetics, binding sites and reactivity of the Pt-protein adducts of cisplatin and transplatin towards biological nucleophiles, *J. Inorg. Biochem.*, 2002, 91 (1), 306–311.
88. Y. Najajreh, T. P. Shulman, O. Moshel, N. Farrell and D. Gibson, Ligand effects on the binding of cis- and trans-[PtCl(2)Am1Am2] to proteins, *J. Biol. Inorg. Chem.*, 2003, 8 (1-2), 167–175.
89. C. S. Allardyce, P. J. Dyson, J. Coffey and N. Johnson, Determination of drug binding sites to proteins by electrospray ionisation mass spectrometry: the interaction of cisplatin with transferrin, *Rapid Commun. Mass Spectrom.*, 2002, 16 (10), 933–935.
90. A. Casini, C. Gabbiani, G. Mastrobuoni, L. Messori, G. Moneti and G. Pieraccini, Exploring metallodrug-protein interactions by ESI mass spectrometry: the reaction of anticancer platinum drugs with horse heart cytochrome c, *ChemMedChem*, 2006, 1 (4), 413–417.
91. A. Pattanaik, G. Bachowski, J. Laib, D. Lemkuil, C. F. Shaw, D. H. Petering, A. Hitchcock and L. Saryan, Properties of the reaction of cis-dichlorodiammineplatinum(II) with metallothionein, *J. Biol. Chem.*, 1992, 267 (23), 16121–16128.
92. S. D. Tsotsoros, Y. Qu and N. P. Farrell, The reaction of dichlorodiammineplatinum(II), [PtCl2(NH3)(2)], isomers with zinc fingers, *J. Inorg. Biochem.*, 2015, 143, 117–122.
93. J. L. Apuy, X. H. Chen, D. H. Russell, T. O. Baldwin and D. P. Giedroc, Ratiometric pulsed Alkylation/Mass spectrometry of the cysteine pairs in individual zinc fingers of MRE-Binding transcription factor-1 (MTF-1) as a probe of zinc chelate stability, *Biochemistry*, 2001, 40 (50), 15164–15175.
94. B. Zhang and W. Tang, Kinetics of the reaction of platinum(II) complexes with metallothionein, *J. Inorg. Biochem.*, 1994, 56 (3), 143–153.

95. M. I. Djuran, E. L. M. Lempers and J. Reedijk, Reactivity of chloro(diethylenetriamine)platinum(II) and aqua(diethylenetriamine)platinum(II) ions with glutathione, s-methylglutathione, and guanosine 5'-monophosphate in relation to the antitumor-activity and toxicity of platinum complexes, *Inorg. Chem.*, 1991, 30 (12), 2648–2652.
96. A. Krężel and W. Maret, Dual nanomolar and picomolar Zn(II) binding properties of metallothionein, *J. Am. Chem. Soc.*, 2007, 129 (35), 10911–10921.
97. A. Drozd, D. Wojewska, M. D. Peris-Diaz, P. Jakimowicz and A. Krężel, Crosstalk of the structural and zinc buffering properties of mammalian metallothionein-2, *Metallomics*, 2018, 10 (4), 595–613.
98. G. Westin and W. Schaffner, A zinc-responsive factor interacts with a metal-regulated enhancer element (MRE) of the mouse metallothionein-I gene, *EMBO J.*, 1988, 7 (12), 3763–3770.
99. X. Chen, M. Chu and D. P. Giedroc, MRE-Binding transcription factor-1: weak zinc-binding finger domains 5 and 6 modulate the structure, affinity, and specificity of the metal-response element complex, *Biochemistry*, 1999, 38 (39), 12915–12925.
100. J. H. Laity and G. K. Andrews, Understanding the mechanisms of zinc-sensing by metal-response element binding transcription factor-1 (MTF-1), *Arch. Biochem. Biophys.*, 2007, 463 (2), 201–210.
101. Y. Li, T. Kimura, J. H. Laity and G. K. Andrews, The zinc-sensing mechanism of mouse MTF-1 involves linker peptides between the zinc fingers, *Mol. Cell. Biol.*, 2006, 26 (15), 5580–5587.